Universitätsklinikum Hamburg-Eppendorf

Zentrum für Experimentelle Medizin, Institut für Tumorbiologie

Direktor: Prof. Dr. med. Klaus Pantel

Wissenschaftliche Betreuung: Prof. Dr. Steven A. Johnsen

Role of H3K27me3 demethylases JMJD3 and UTX in differentiation of mesenchymal stem cells

Dissertation

zur Erlangung des Grades eines Doktors der Medizin

an der Medizinischen Fakultät der Universität Hamburg.

Vorgelegt von:

Carolin Springborn

aus Hamburg

Hamburg 2019

Angenommen von der Medizinischen Fakultät der Universität Hamburg am: 29.05.2019

Veröffentlicht mit Genehmigung der Medizinischen Fakultät der Universität Hamburg.

Prüfungsausschuss, der Vorsitzende: Prof. Dr. Klaus Pantel

Prüfungsausschuss, zweiter Gutachter: Prof. Dr. Thorsten Schinke

Table of content

Introduction

Mesenchymal stem cells

Stem cells are characterized by the unique potential to develop into different types of cells and tissues in the body. Moreover, due to high proliferative potential these cells maintain the pool of stem cells within the body. Depending on the differentiation potential stem cells can be classified into different types. Embryonic stem cells (ESCs), derived from the inner cell mass of a blastocyst are pluripotent. They have the potential to develop into all cell types of the three germ layers. Unlike ESCs, adult stem cells have a limited differentiation potential. They can be found during the whole lifetime of a living organism. Their role is to maintain and repair the tissue they are specific for.

There are two different types of adult stem cells in the bone marrow, the blood progenitor cells or the so called hematopoietic stem cells, and bone marrow stromal cells or mesenchymal stem cells (MSCs). Pioneering work was done by Friedenstein and coworkers who firstly isolated bone-forming progenitors from rat bone marrow in 1960ies (Friedenstein & Petrakova, 1966). MSCs contribute to connective tissue formation, regeneration and maintenance. MSCs are multipotent and can differentiate only into limited number of cell types which are among others osteoblasts, adipocytes and chondrocytes (Caplan, 1991; Pittenger, 1999).

MSCs can be obtained from bone marrow aspirates and based on their ability to selectively adhere on plastic they can be easily propagated in culture. Moreover, it has been shown that MSCs have the potential to migrate and circulate in the peripheral blood, however collecting sufficient number of cells for culturing from blood is a complicated task (Kassis, et al., 2006). MSCs can also be found in non-marrow tissues like adipose tissue, muscle, umbilical cord blood and tissue (Wharton's jelly) as well as placenta (Wagner, et al., 2005; Veryasov, et al., 2014). After isolation cells need to be selected based on combination of three criteria that are MSC specific. Firstly, as mentioned before MSCs are plastic-adherent in standard culture conditions, where they form fibroblast-like colonies. Secondly, they show a typical pattern of positive expression of surface markers CD73, CD90 and CD105 and lack expression of CD14, CD34, CD45 or CD11b, CD79alpha or CD19 and HLA-DR. The final criterion is the ability to differentiate into several mesenchymal lineages such as adipocytes, chondroblasts and osteoblasts in vitro (Dominici, et al., 2006).

The process of MSC differentiation consists of two steps which are lineage commitment to specific progenitors, followed by the development into specific cell types, called maturation. A number of signaling pathways control lineage commitment such as wingless-type MMTV integration site (Wnt) signaling, transforming growth factor-beta (TGFβ)/bone morphogenic protein (BMP) signaling, Hedgehogs (Hh) (Cheng, et al., 2012; Lin & Hankenson, 2011; Kim, et al., 2010). Furthermore, serving as direct or indirect targets of signaling pathways, transcription factors initiate and define the lineage-specific differentiation. A key factor associated with osteoblast differentiation and skeletal morphogenesis is runt-related transcription

factor 2 (RUNX2) (Komori, 2005). Upregulation of RUNX2 promotes osteoblastic differentiation potential and was shown to inhibit adipocyte differentiation (Komori, 2010). RUNX2 activates promoters and induces expression of bone matrix protein genes like osteocalcin, collagen type 2 (Col2a1), bone sialoprotein (BSP) and Osteopontin (OPN) in immature and mature osteoblasts (Ducy, et al., 1997; Zheng, et al., 2004; Sato, et al., 1998). Another important transcription factor involved in osteoblast differentiation and specifically required for maturation is Osterix. It was found to act downstream of RUNX2 (Nakashima , et al., 2002).

A large number of signaling factors are similarly involved in regulation of adipogenic differentiation. Namely, members of BMP and Wnt signaling pathway play also a crucial role here in lineage commitment (Haiyan, et al., 2009; Bennett, et al., 2002). Moreover, differentiation inducing factors like insulin-like growth factor 1 (IGF1), glucocorticoids and cAMP are equally relevant for adipocyte formation and maturation (Boucher, et al., 2010). In addition, the key transcription factors involved in initiation and maintenance of adipogenic lineage commitment are members of the CCAAT/enhancer-binding protein (C/EBP) family (Gregoire, et al., 1998). In response to inducing signaling C/EBPβ and C/EBPδ are upregulated within a few hours and start the induction of adipocyte differentiation. C/EBPβ in turn activates C/EBPα and the transcription of nuclear receptor peroxisome proliferator–activated receptor γ (PPARG) (Tang & Lane, 2012). PPARG is another master regulator of adipocyte differentiation. (Rosen, et al., 1999). C/EBPα maintains the expression of PPARG and both work together regulating expression of a number of adipocyte-specific genes.

The application of MSCs in medicine

MSCs have a wide range of functions and are targets for different approaches in regenerative medicine. MSCs are indispensable for the renewal of the tissue during growth and aging process or while injuries and diseases. It was discovered that MSCs have immunomodulatory and immunosuppressive functions. MSCs inhibit B-cell proliferation and differentiation and suppress monocyte differentiation into dendritic cells (Corcione, et al., 2006; Xiao-Xia, et al., 2005). Furthermore, they secrete soluble factors like transforming growth factor-β, prostaglandin E2, IL- 10 an IL-6, which suppress an immune response by modulating T-cell activation and proliferation. These facts offer a potential therapeutic use of MSCs in immune-mediated diseases and could be useful to prevent immune rejections of organ transplants and graft-versus-host disease (Nicola, et al., 2002; Bartholomew, et al., 2002; Le Blanc, et al., 2004). Moreover, the ability to differentiate into several lineages of the mesenchymal tissue offers new possibilities in tissue engineering and transplantation-based therapy.

It has been reported that MSCs can be recruited to the sites of injured tissues as well as to tumors, where they build an optimal microenvironment for tumor cells. MSCs are attracted to these sites mainly by inflammatory mediators. Large number of publications have pointed out the ability of bone-marrow derived MSCs to home different solid tumors such as colon (Shinagawa, et al., 2010), prostate (Jung, et al., 2013), pancreas (Beckermann, et al., 2008) and breast (Karnoub, et al., 2007), as well as metastatic tumors. Due to their tumor homing property, MSCs are an interesting and promising tool for cancer therapy. As MSCs are

easy to isolate and show great differentiation potential they can be easily transduced by vectors to serve as a vehicle for therapeutic agents (Serakinci, et al., 2011).

Understanding the regulatory mechanisms controlling the lineage commitment of MCS is also crucial for treatment of osteopathologies. Of a current interest are the ageing associated conditions which progressed rapidly over last decades because of the phenomenon of world population ageing. The most prevalent bone disease nowadays among aged population is osteoporosis, bone loss induced by increased rate of bone resorption and reduced rate of bone formation. This leads to reduced bone density and quality which then very often results in fractures with subsequent defects and/or delays in fracture healing. There is only poor current data about prevalence and incidence of osteoporosis and osteoporosis related fractures in Germany. Last update was in 2009 Bone Evaluation Study (BEST), a retrospective analysis health insurance data revealed that 14% of insurees in the age of 50-99 had osteoporosis. Extrapolation on the German population reveals a prevalence of 17% or 6.3 million people and an incidence of 2.1% in 2009. Among all insured persons that were diagnosed to have osteoporosis, every second sustained fractures in the 3 year observation period (Hadji , et al., 2013). Women are usually more affected because of the menopause associated lack of estrogen which is an important regulator of bone remodeling. Although the mechanistic steps leading to osteoporotic phenotype are well characterized it is little known about the particular steps of pathogenesis. Interestingly, during osteoporosis very often differentiation of MSCs is misregulated and shifted in favor of adipogenesis and less osteoblast formation. This could be the leading mechanism of bone marrow adiposity observed during osteoporosis. Cell fate determination pathways involve very complex and intricate transcriptional and epigenetic programs. Understanding and exploring the key mechanisms that control differentiation of MSCs into osteoblasts and adipocytes would clarify the possible approaches that could be used as a potential basis for newer and better therapies of age-related osteoporosis (Pino, et al., 2012).

Epigenetic modifications

Although all cells of an organism are genetically identical, i.e. they carry the same DNA content, the cells of different tissues completely differ from each other in their shape, structure and functions within the same organism. These changes are achieved through the differential expression of gene signatures that define the fate and ‘identity’ of the cell. The gene expression changes can be regulated through many different ways, including those controlled by epigenetic programs. Epigenetics focusses on regulation mechanisms of gene activity that does not involve changes in the DNA sequence itself but happens ‘above’ the genetic level. In fact, epigenetic changes modify the chromatin structure and DNA accessibility to transcription factors and enzymes that are responsible for gene transcription. The most important epigenetic mechanisms include RNA interference, chromatin remodeling, DNA methylation and histone modifications.

Chromatin organization

The human genome consists of approximately 3.2 x 10^9 nucleotides spread over 23 chromosomes. Every chromosome is composed of a long DNA molecule packed and folded by proteins into a tight and compact structure. This complex of protein and DNA is called chromatin (from 'chroma' which is Greek, meaning 'colour' because of its staining properties). Chromatin is the highest condensed form of DNA, consisting of a coalition of negatively charged DNA, wrapped around positively charged histones, as well as other proteins that attached to the DNA (Alberts, et al., 2002).

The basic unit of chromatin is a nucleosome which is a complex of an octamer of histones made up of two molecules of the histone H2A, H2B, H3 and H4 and 147 base pairs of DNA wrapped around them. Histone H1 does not contribute to nucleosome formation but connects the particular nucleosomes to each other. The next bigger unit is the 30nm fiber built by 6 nucleosomes. Non-histone proteins further condensate and pack the fiber so tightly, that the DNA is less accessible for transcription factors and gene expression is reduced (Kornberg, 1974; Widom, 1998). Depending on the grade of condensation and the accessibility of DNA, there are two different states of chromatin. Less condensed, active euchromatin with a higher density of expressed genes and highly condensed, less transcriptionally active heterochromatin, containing fewer expressed genes (Mello, 1983). Compact states are important for cell division and distribution of DNA whereas lightly packed form of chromatin is required for DNA transcription and replication.

All histones have a core domain and a C- and N-terminus tail. The histone tails lie at the surface of nucleosome. Thus, they are easily accessible and become post-translationally modified in various ways (Jenuwein & Allis, 2001). The modifications, such as phosphorylation, acetylation or methylation can directly or indirectly alter chromatin structure to facilitate transcriptional activation or repression, respectively. Histone methylation occurs on all basic residues: lysines, arginines and histidines. Furthermore, there exist whole proteins like ubiquitin that act as a histone modification (Jenuwein & Allis, 2001; Johnsen, 2012). It was discovered that chromatin confirmation and accessibility can change depending on the different type of present histone modifications. This brought up the idea of the so called "histone code" (Strahl & Allis, 2000). Trimethylation of lysine 27 of histone H3 by polycomb group proteins (PcG) for example leads to a repressive state of chromatin associated with inactivation of gene expression. Other epigenetic modifications associated with gene silencing are di- and trimethylation of H3K9 and methylation of H4K20. Transcriptionally active chromatin is mainly marked by histone acetylation and for example methylation of H3K4, H3K79 or H3K36 (Kouzarides, 2007).

Chromatin bivalency

It is thought that some genes are epigenetically tagged with markers for both, transcriptional activation and repression, such as H3K4me3 and H3K27me3, respectively. H3K4me3 mark is mainly located at transcription start sites (TSS) and associated with active promoters (Mikkelsen, et al., 2007). But it can be

also found together with repressive mark H3K27me3 on transcriptionally silent promoters. The discovery of the coexistence suggested that these 'bivalent' marks keep the promoter in a balanced-state. Depending on the incoming signal this state of bivalency can be resolved in favor of either gene activation or further repression (Bernstein, et al., 2006).

Genome-wide mapping studies of chromatin modifications could show that most of the differentiation-specific genes in human embryonic stem cells (hESCs) are bivalent. (Pan, et al., 2007; Noer, et al., 2009; Bernstein, et al., 2006). In case of gene activation, H3K27me3 is removed while H3K4me3 mark remains, followed by RNA polymerase recruitment and start of the transcription. On the contrary, during gene repression H3K4me3 is removed and H3K27me3 remains, leading to recruitment of silencing complexes. Most of the research done on bivalency was performed in ES cells, however similar regions with bivalent histone modification domains were also found in differentiated human T cells (Roh, et al., 2006). Furthermore, the work done by our group showed that human MSCs (hMSCs) also exhibit a state of bivalency on the adipocyte-specific genes which is resolved via a loss of H3K27me3 upon differentiation (Karpiuk, et al., 2012).

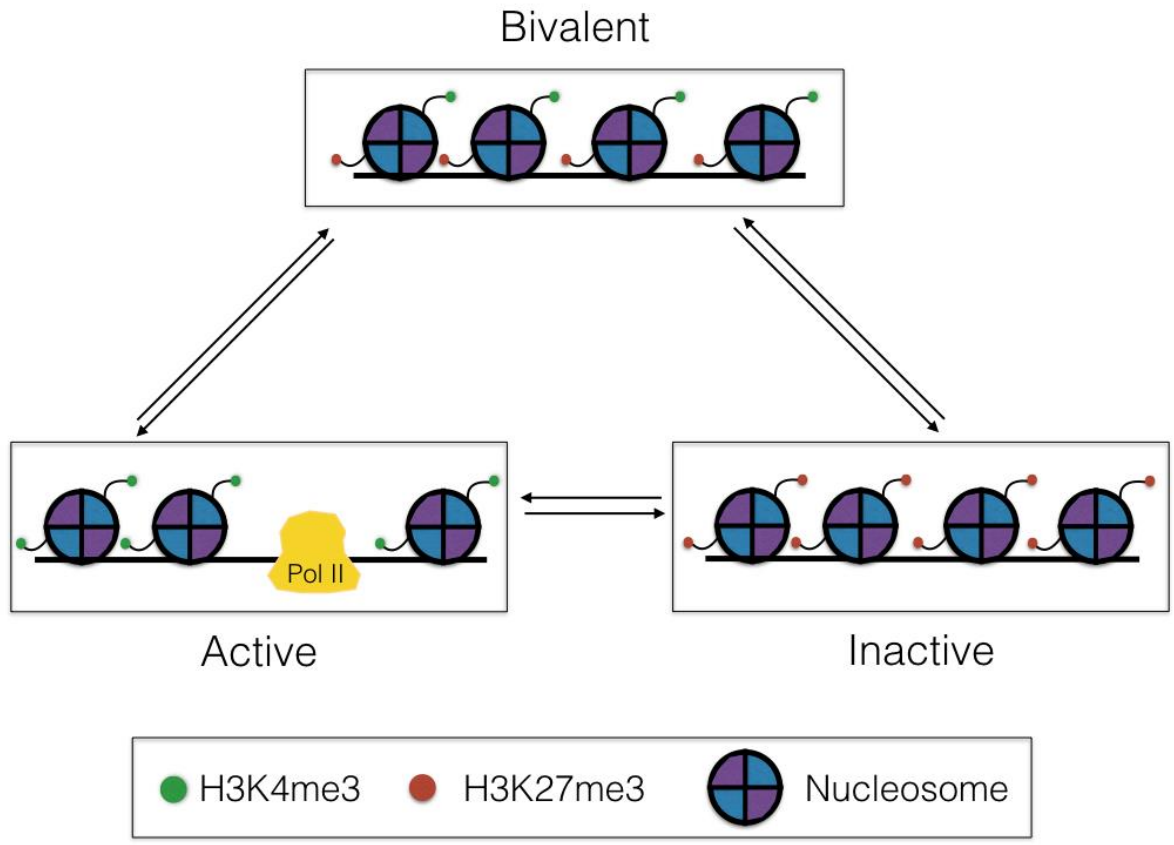

Figure 1. Gene bivalency. There are three different states of gene expression dependent on histone methylation. Active state is associated with high levels of H3K4me3 (green) and active gene transcription by RNA-Polymerase II (POL II). Genes in the bivalent state have both H3K4me3 and H3K27me3 (red) marks whereas the repressive or inactive mode is characterized by high levels of H3K27me3 and loss of H3K4me3.

Histone H3 Lys 27 trimethylation

Histone H3 Lys 27 trimethylation (H3K27me3) is a repressive histone modification mediated by the polycomb group (PcG) proteins. PcG proteins are subdivided into two protein complexes: Polycomb repressive complex 1 (PRC1) (Saurin, et al., 2001) and Polycomb repressive complex 2 (PRC2) (Kuzmichev, et al., 2002; Muller, et al., 2002). Both protein complexes repress a plethora of genes in embryonic stem cells, including many transcriptional regulators important for development (Boyer, et al., 2006). While PRC1 is known to inhibit chromatin remodeling in Drosophila embryos (Shao, et al., 1999), PRC2 catalyzes methylation of lysine 27 on histone H3 (H3K27me, me2 and me3) (Ferrari, et al., 2014). We know less about the mono- and dimethylated state of H3K27 but it could be shown that H3K27me1 is associated with active promoters whereas di- and trimethylation of H3K27 lead to promoter repression and inactive gene transcription (Barski, et al., 2007). In mammalian cells, PRC2 includes four subunits: histone-lysine N-methyltransferase EZH2, suppressor of zeste 12 (SUZ12), Embryonic ectoderm development protein (EED) and the histone binding protein retinoblastoma-binding protein p48 (RbAp48). Forming the catalytic subunit of PRC2, SET domain of EZH2 is able to methylate Lysin-9 of histone 3 (H3K9me) as well as Lysin-27 of the same histone (H3K27me,-mr2,-me3) (Cao, et al., 2002). It was found that mutation of SET domain leads to a loss of H3K27me3 (Muller, et al., 2002). For normal embryonic development, all core components of PRC2 are indispensable. It could be shown that a loss of one of the components is usually lethal at the stage of gastrulation.

The counterpart of EZH2 is built by the histone demethylases UTX (KDM6A) and JMJD3 (KDM6B) that are able to offset the repressive action of H3K27me3. They belong to a small group of JmjC-domain enzymes that have antagonistic functions to PRC2. By removing the methyl group of H3K27, UTX and JMJD3 play an essential role for gene regulation and regular differentiation (Agger, et al., 2007).

Cellular functions and the role of H3K27me3 in diseases

The Polycomb Group (PcG) induced trimethylation of H3K27 was identified to repress homeotic gene loci (HOX) in Drosophila (Schuettengruber , et al., 2007; Simon & Kingston RE, 2009). This hints to the crucial role of PcG in the embryonic development and regulation of the anterior-posterior axis. Furthermore, it was established that EZH2 is overexpressed in several solid tumors like for example prostate cancer (Varambally, et al., 2002). While EZH2 downregulation leads to decreased proliferation of breast cancer cells, high levels of EZH2 were detected in aggressive forms of breast cancer which might offer a new possibility in detecting early aggressive malignant breast tumors and serve as a prognostic determinant of patients' survival (Gonzalez, et al., 2009; Kleer, et al., 2003). Recently, the transcription-repressive property of H3K27me3 was further examined in the context of various human cancer development and progression, such as breast, pancreatic and ovarian cancer. In a work from Wei et al. it was found that trimethylation of H3K27 was lower in tumor tissue of breast, pancreatic and ovarian cancer, compared to adjacent non-malignant healthy tissue (Wei, et al., 2008). Moreover, activating point mutations in EZH were discovered in B cell lymphoma (Visser, et al., 2001)

Cell fate determination and differentiation of mesenchymal stem cells is, among others, also influenced by H3K27me3. Investigation of genome-wide distribution of EZH2 in non-differentiated MSCs and osteoblast-differentiated MSCs demonstrated that, out of more than 4000 genes bound by EZH2 less than 30 maintain it after induction of differentiation. This implies that MSCs exhibit a loss of H3K27me3 in favor of activation of differentiation related genes (Wei, et al., 2011).

Dynamic histone methylation and demethylation were discovered to play also an important role in ageing of adult tissue-specific stem cells. Adult tissue stem cells are essential for tissue regeneration and repair as well as for tissue maintenance. It was suggested that an imbalance of stable and dynamic methyl marks led to a decline of tissue function as reviewed in (Pollina & Brunet, 2011). Interestingly, in patients with Hutchinson-Gilford Progeria Syndrome (HGPS), a genetic premature aging disease related to loss of heterochromatin, was accompanied by a loss of H3K27me3 on the inactive X-chromosome as well as a decrease in methyltransferase EZH2 levels (Shumaker, et al., 2006). Because of these observations it can be assumed that a decrease in heterochromatin and the resulting subsequent misregulation of gene expression plays a crucial role during ageing.

Histone demethylases UTX (KDM6A) and JMJD3 (KDM6B)

Genome-wide chromatin immunoprecipitation (ChIP) sequencing in ESCs could show that EZH2-mediated H3K27me3 occupies promoters of genes that are relevant for differentiation (Boyer, et al., 2006). After this discovery, large proportion of research concentrated on elucidating the mechanisms of H3K27me3 removal from chromatin to address the question of how activation of lineage specific genes can be regulated. At that time, two histone H3K27me3 demethylases-Lysine (K)-Specific Demethylase 6A and 6B (KDM6A/B), or UTX and JMJD3 respectively, were discovered.

In the initial studies it was found that UTX, which escapes X chromosome inactivation in females, plays a critical role in posterior development in zebrafish. Moreover, it was found that UTX is localized at the transcriptional start site of the HOX genes (Lan, et al., 2007). KDM6A builds a complex with mixed-lineage leukemia 2 (MLL2) which forms the catalytic active part of trithorax group (trxG) of proteins (Greenfield, et al., 1998). MLL 2 acts as methyltransferase specific for histone 3 lysine 4, (Lee, et al., 2007). Active H3K4me3 and repressive H3K27me3 are often co-localized at the same promoters keeping them in balance and hence the gene in ‘poised’ state. In case of MLL 2 and UTX, the bivalent chromatin marks would be resolved due to addition of active and removal of repressive mark, respectively enabling induction of gene expression (Schuettengruber, et al., 2011). Van Haaften et al. discovered inactivating somatic mutations of UTX in several types of cancer, such as multiple myeloma, esophageal and renal cancer. Furthermore they demonstrated that reintroduction of UTX into tumor cells decreased H3K27me3 at PcG target genes, leading to reduced cell proliferation (van Haaften, et al., 2009). Mutations in MLL 2/UTX complex were also found to appear in transitional cell bladder cancer as well as in pediatric medulloblastoma and in Kabuki syndrome, a congenital anomaly (Gui, et al., 2011; Dubuc, et al., 2013; Miyake , et al., 2013). In mice, homozygous UTX mutations were found to be mid-gestational lethal and show defects in neural tube as well as an

insufficient cardiac development, indicating that UTX is essential for embryonic development (Shpargel, et al., 2012). Additionally, the role of UTX in cardiac development was further strengthen by the inability of UTX-deficient ESC's to generate heart-like rhythmic contractions (Lee, et al., 2012).

Homolog to UTX is UTY (KDM6C) which is located on the Y chromosome and thus only expressed in male organisms. It could be demonstrated that UTY has overlapping functions compared to UTX in embryonic development. In vitro studies showed that UTY has no demethylase characteristics (Lan, et al., 2007), whereas amino sequence analysis of both reveals a high sequence similarity (88% in humans and 82% in mice). Inspired by this fact Shpargel et al. revealed that UTY compensates the loss of UTX in male embryo apart from demethylase mechanisms (Shpargel, et al., 2012).

JMJD3 or Lysine (K)-Specific Demethylase 6B (KDM6B), promotes transcriptional elongation by building a complex with KIAA1718, a specific demethylase of H3K9me2, H3K27me2 and H4K20me1. This complex facilitates the recruitment of proteins involved in elongation like Spt 6, Spt 16, SETD2, CHD7 and CDC73, partially controls the release of paused RNA Polymerase II to active form and supports RNA Pol II progression along the gene (Chen, et al., 2012; Estarás , et al., 2013). As KIAA1718 contains a plant homeodomain (PHD) that can bind trimethylated H3K4 it could possibly pave the way for a bivalent regulation of gene expression on a epigenetic chromatin level (Horton, et al., 2010; Voigt, et al., 2013). JMJD3 was found to play role in many differentiation processes like determining cell fate choice of embryonic stem cells towards neural lineage (Burgold, et al., 2008) and macrophages in inflammatory response (De Santa, et al., 2007). A selective jumonji H3K27me3 demethylase inhibitor GSK-J4 discovered by Kruidenier et al., reduced lipopolysaccharide-induced proinflammatory cytokine production by macrophages (Kruidenier, et al., 2012). Furthermore, reactivation of herpes simplex virus 1 in trigeminal ganglion neurons was inhibited in vitro with the treatment of the previously mentioned inhibitor (Messer, et al., 2015).

Recently, it was shown that KDM6B and H3K9 demethylase KDM4B regulate differentiation of human bone marrow MSCs towards the osteogenic lineage. It was suggested that both demethylases play a role in mediating BMP-signaling-induced bone formation. Furthermore, downregulation of KDM4B and KDM6B led to reduced osteogenic differentiation and increased adipogenesis. The ovariectomized and aging mice, with high bone-marrow adiposity, displayed higher content of H3K27me3 and H3K9me3-positive MSCs in the bone marrow (Ye, et al., 2012). Similarly, knockdown of UTX gene in hMSCs resulted in increased adipogenesis and decreased osteogenesis, while EZH2 knockdown showed opposite effects (Hemming, et al., 2014). As JMJD3 is known to be a target of many microRNAs it was currently discovered that microRNA MIR146A functions as a negative regulator of JMJD3 (Lewis, et al., 2005). Interestingly, the overexpression of MIR146A in hMSCs resulted in decreased JMJD3 and an increase in H3K27me3 leading to increased levels of runt-related transcription factor 2 (RUNX2), a marker of osteogenic differentiation (Huszar & Payne, 2014).

Altogether, modulation of the activity of histone demethylases JMJD3 and UTX offers a new possibility for controlling MSC differentiation towards desired lineage which might present new therapeutic strategy in the treatment of bone diseases amongst others.

Aim of the project

Epigenetic regulation plays a central role in controlling cell phenotype. Previous work from our group has demonstrated that dynamic changes in post-translational modifications of histone proteins are essential for the differentiation of multipotent human mesenchymal stem cells to the adipocyte and osteoblast lineage. In particular, adipocyte-specific genes exist in a bivalent epigenetic state containing markers for both transcriptional activation and repression. Upon the induction of differentiation these genes exhibit a loss of the repressive mark (trimethylation of lysine 27 of histone H3; H3K27me3), while not changing or increasing the amount of the positive mark H3K4me3. However, the mechanisms controlling the transition between the bivalent and active (or repressed) states is largely unknown. We hypothesize that active demethylation of H3K27 via one of the known histone demethylases JMJD3 (KDM6B) or UTX (KDM6A) is required for hMSC differentiation. In order to address this hypothesis, we utilized a cell culture-based approach with a telomerase-immortalized hMSC cell line. The functional relevance of JMJD3 and UTX during MSC differentiation was assessed through selective inhibition as well as through siRNA induced depletion of these proteins. Gene expression studies, stainings (Oil Red O for adipocytes, alkaline phosphatase for osteoblasts) and Western Blot analysis were performed to evaluate the effect of JMJD3 and/or UTX inhibition/loss during differentiation of hMSCs into adipocytes and osteoblasts. In order to get an overall picture of the role of JMJD3 in differentiation of hMSCs, in particular, we analyzed transcriptome wide gene expression changes following JMJD3 knockdown.

Material and Methods

Cell culture and differentiation

Tert-immortalized human mesenchymal stem cells T20 (splitted in1:20 ratio) and T4 (splitted in 1:4 ratio) were obtained from Prof. M. Kasem's lab in Odense, Denmark (Simonsen, et al., 2002). They were cultured in alpha-MEM medium, supplemented with 10 % fetal bovine serum (FBS) (Lonza) and 1 % antibiotic/antimycotic (Sigma Aldrich). To induce adipocyte differentiation 100 nM dexamethasone, 0.45 mM isobutylmethyl-xanthine (AppliChem, Biochemica), 2x 10-6 insulin (Sigma Aldrich) and 10 µM troglitazone (LKT Laboratories, Inc.) were added to normal growth medium. For osteoblastic lineage differentiation growth medium was supplemented with 100 nM dexamethasone (Serva Electrophoresis GmbH), 10 mM β-glycerophosphate (Sigma Aldrich), 0.2 mM L-ascorbatic acid (Sigma Aldrich), 10 nM calcitriol.

siRNA Transfection

siRNA sequences that were used in the project are listed in Table1. First of all, transfection mix consisting of 500 µl OptiMEM (Invitrogen, Gibco), 4 µl of RNAiMAX (Invitrogen) and 1µl of siRNA was prepared and incubated for 20 minutes at room temperature (amount used for 1 well of a 6 well plate). While incubation time, MSCs were washed and trypsinized. Trypsin was blocked with growth media without antibiotic/antimycotic. Next cells were counted and distributed on a 6- or 12-well plate (200.000 cells/well of a 6-well plate). 500 µl of transfection mix was added to cells and the volume was brought up to 2 ml by adding medium without antibiotic/antimycotic. After 24 hours medium was changed to normal medium and differentiation was induced as described above. If necessary, cells were retransfected after 72 hours by forward transfection.

Table 1. **siRNA sequences used in the study**

Target name	**Serial number**	**Sequence of the sence strand**	**Manufacturer**
Control siRNA Luciferase GL2 Duplex	D-001100-01-2	CGTACGCGGAATACTTCGA	Dharmacon
JMJD3/KDM6B siGENOME smart pool	D-023013-01 D-023013-02 D-023013-03 D-023013-04	GGAAUGAGGUGAAGAACGU GGAGACCUCGUGUGGAUUA CCACAGCGCCCUUCGAUAC GCACAAACGGAACUAUGGA	Dharmacon
UTX/KDM6A siGENOME smart pool	D-014140-01 D-014140-02 D-014140-04 D-014140-05	GAACAGCUCCGCGCAAAUA GAGAGUAAUUCACGAAAGA CAGCACGAAUUAAGUAUUU GCUAUUGGCUGGUGCAACA	Dharmacon

Inhibitor treatment

GSK-J4 (*N*-[2-(2-Pyridinyl)-6-(1,2, 4,5-tetrahydro-3*H*-3-benzazepin-3-yl)-4-pyrimidinyl]-β-alanine ethyl ester) a prodrug which is hydrolyzed to GSK-J1 which is a selective inhibitor of JMJD3 and UTX. Inhibitor was purchased from Tocris (Cat. No. 4594). For inhibitor treatment MSCs were pretreated with 1µM of GSK-J4 diluted in ethanol for 2 hours. Afterwards, cells were induced to differentiate for 5 days. Medium including differentiation factors and 1µM of inhibitor was renewed daily. To the control group of MSCs, equal volume of ethanol was added.

Protein Extraction and Western Blot

Cells were lysed in RIPA buffer (1x PBS, 1 % Nonyl Phenoxypolyethoxylethanol 40, 0.5 % Sodium Deoxycholate, 0.1 % Sodium Dodecyl Sulfate) supplemented with protease inhibitors (10 mM β-glycerophosphate, 10 mM N-Ethyl Maleimide, 10 nM Pefabloc, 1 mM Aprotinin/ Leupeptin). Next, cells were scraped and the suspension was transferred into Eppendorf tubes. Samples were sonicated for 2 times 15 seconds. The 6x Laemli buffer was added and protein samples were denatured at 95 °C for 5 minutes. Using SDS-polyacrylamide gel electrophoresis, proteins were separated (20 mA, maximum voltage) and transferred on a nitrocellulose membrane (Whatmann) (100 V, maximum current for 90 minutes). To block proteins, the membrane was washed in 5 % milk in TBST for at least 1 hour. The blots were incubated with primary antibody (listed in Table 2) dilutions in 5 % milk diluted in TBST overnight at 4 ˚C. The next day the membrane was washed 3 times 10 minutes in TBST. Thereafter, the membranes were incubated for another hour at RT in dilutions of secondary antibodies coupled with HRP in 5 % milk. Following this incubation, the membrane was again washed in TBST 3 times for 10 minutes. Blots were developed using chemiluminescent HRP substrate (Immobilon Western, Millipore) or SuperSignal WestFemto Maximum Sensitivity Substrate (Thermo Scientific).

Table 2. **Antibodies used for Western Blot**

Name of Antibody	**Dilution factor**	**Catalogue number**	**Source**
HSC70	1:30000	Sc-7298	Santa Cruz
JMJD3 (KDM6B)	1:1000	MBS 150629	MyBioSource
UTX (KDM6A)	1:1000	A302-374A	Bethyl
H2B	1:10000	Ab52484	Abcam
H3K27me3	1:1000	C15410195	Diagenode

Alkaline Phosphatase Staining

Alkaline phosphatase dye kit was purchased from Sigma Aldrich. Before staining, cell fixation solution containing citrate solution, acetone and 37 % formalin (5:13:1.6) and alkaline dye solution was prepared. For dye solution 5 mg Naphtol Phosphate Disodium Salt was dissolved in 200 µl N, N-Dimethylformamide and added into 50 ml 0.1 M Tris-HCl (pH 8.5). The mixture was further supplement with 30 mg of Fast Blue

RR Salt (Sigma Aldrich) and whole dye solution was filtered. Next, cells were washed once with PBS, fixed for 30 seconds with the prepared fixation solution and washed with deionized water for 45 seconds. Finally 1ml of alkaline phosphate dye solution was added to the cells and they were incubated for 15-30 minutes at room temperature in the dark. At last, dye was removed and cells were washed and allowed to dry.

Oil Red O Staining

Growth medium was removed, cells were washed with PBS and 10 % formalin in PBS was added to the cells for fixation. During the incubation time of 30 minutes, staining solution consisting of 3 parts of Oil Red O stock (300 mg Oil Red O powder, Sigma Aldrich, dissolved in 100 ml of 99 % isopropanol) and 2 parts of deionized water was prepared. Dye solution was incubated for 10 minutes at room temperature and filtered. After fixation, formalin was removed and cells were washed with deionized water. 60 % of isopropanol was added and incubated for 5 minutes. Prepared Oil Red O solution was added to the cells after removing isopropanol. Cells were kept for 5-10 minutes in dye solution and finally washed several times with deionized water. Plates were dried and staining was analyzed under light microscope.

RNA Isolation

Cells were washed with PBS and 500 µl Qiazol Lysis Reagent (Qiagen) per well of a 6-well plate was added. After 2 minutes of incubation on the shaker, cells were scraped and suspension was transferred to an Eppendorf tube. After 5 minutes of incubation at room temperature, tubes were kept on ice. 100 µl of chloroform was added and the suspension was vortexed thoroughly for 30 seconds. Then, tubes were centrifuged for 20 minutes at 10000 rpm at 4 °C and the top layer of clear aqueous phase was transferred into a new tube, kept on ice. 500 µl of chloroform was added and samples were vortexed and centrifuged again for 15-20 minutes under same conditions. Supernatant was transferred into new Eppendorf tubes and an equal amount of isopropanol was added. Samples were kept at -20 °C overnight. Next day samples were vortexed and centrifuged 20 minutes at 12000 rpm, 4 °C. The supernatant was removed and the remaining pellets were washed two times with 70 % ethanol by vortexing and centrifugation. Thereafter, pellets were dried on SpeedVac for 5 minutes. To resuspend the pellets, 30 µl of Diethylpyrocarbonate (DEPC) water was added and samples were vortexed briefly 2 times for 1 minute. RNA concentration was measured with Nanodrop Spectrophotometer. If necessary, samples were further purified by adding 1/10 volumes of 3 M sodium acetate (pH 5.2) and 2.5 volumes of 100% ethanol. After 15 minutes of centrifugation at 13000 rpm at 4 °C, the supernatant was removed and washing, drying and resuspension was repeated.

Reverse transcription

1 µg of total RNA was brought up to a volume of 10 µl by DEPC water. 2 µl of random primers (Sigma Aldrich) and 4 µl of desoxynucleosidtriphosphates (dNTPs) (2.5 mM, Promega) per sample were supplemented and the mix was heated at 70 °C for 5 minutes. After spinning samples 4 µl of a mix consisting of 2 µl 10x Reaction Buffer (NEB), 0.25 µl RNAse inhibitors (10 U, NEB), 125 µl M-MuLV Reverse Transcriptase (25 U, NEB) and 1.625 µl of DEPC water was added. Samples were mixed and spun briefly

before incubation at 42 °C for 1 hour. To inactivate the reverse transcriptase, samples were heated at 95 °C for 5 minutes. Finally reaction mix was diluted by adding 30 µl of DEPC water.

Real-time PCR

A PCR mix consisting of 75 mM Tris-HCl (pH8.8), 20 mM (NH4)2SO4, 0.01 % Tween-20, 3 mM MgCl2, 1:80000 SYBR-Green (Roche), 0.2 mM dNTPs (Promega), 20 U/ml Taq-Polymerase (Primetech, Belorus, 5 U/µl), 10 % Triton X-100 and 300 mM Trehalose was prepared. 14 µl of this PCR mix was brought together with 1.5 µl of reverse and forward primer mix (10 µM) and 8.5 µl deionized H2O and pipetted in a well of a 96-well plate. 1 µl of cDNA was added and relative gene expression was measured on a Thermal Cycler (BioRAD C1000, CFX96) (see thermal profile in *Table 3.*). The results were compared to the standard curve produced by a serial dilution series of cDNA (4-fold) and gene expression was normalized to the expression of housekeeping gene HNRNPK. The expression levels were determined relative to the non-targeting transfected control sample and expressed as relative mRNA expression. The primers used for gene expression analysis are listed in *Table 4*.

Table 3. **Real time PCR thermal profile**

Step	**Temperature, °C**	**Time, minutes: seconds**	**Repetitions**
Initial denaturation	95	2:00	1x
DNA denaturation	95	0:15	40-45x
Primer annealing and elongation	60	1:00	
End	25	2:00	

Melting curve was estimated and detected in 0.5 increments increasing from 60 to 90 degrees.

Table 4. **Primer used for quantitative real-time PCR**

Name	**Sequence**	**Source**
HNRNPK F HNRNPK R	ATCCGCCCCTGAACGCCCAT ACATACCGCTCGGGGCCACT	O. Karpiuk
JMJD3 F JMJD3 R	TCTTGAACAAGTCGGCGTCC CCCCTCACCGCCTATCAGTA	This study
UTX F UTX R	GCAGATTGGGGGCGTCAC TTCATAGCAGCGAACAGC	This study
ALPL F ALPL R	TGGGCCAAGGACGCTGGGAA AAGGCCTCAGGGGGCATCTCG	O. Karpiuk
BGLAP F	GCCCTCACACTCCTCGCCCT	O. Karpiuk

BGLAP R	CGGGTAGGGGACTGGGGCTC	
G6PD F G6PD R	CGACGAAGCGCAGACAGCGTCA CAGCCACATAGGAGTTGCGGGC	O. Karpiuk
RUNX2 F RUNX2 R	GCGGTGCAAACTTTCTCCAG GCAGCCTTAAATGACTCTGTTGG	(Bedi, et al., 2014)
PPARG F PPARG R	ACCTCCGGGCCCTGGCAAAA TGCTCTGCTCCTGCAGGGGG	O. Karpiuk
LPL F LPL R	TCAGCCGGCTCATCAGTCGGT AGAGTCAGCACGAGCAGGGCT	O. Karpiuk
RASD1 F RASD1 R	CAAGACGGCCATCGTGTCGCG GCTGCACCTCCTCGAAGGAGTCG	O. Karpiuk
PDK4 F PDK4 R	TTCACTCCGCGGCACCCTCA TCGGAGCAGAGCCTGGTTCCG	O. Karpiuk
FABP4 F FABP4 R	AAACTGGTGGTGGAATGCGT GCGAACTTCAGTCCAGGTCA	O. Karpiuk

RNA sequencing

Data analysis was kindly performed by the help of Dr. Zeynab Najafov.

To perform RNA-sequencing, intact RNA of very high integrity is needed, therefore we run an aliquot of the RNA-samples on a denaturating agarose gel, stained with ethidium bromide. Library preparation was done using the NEBNext Ultra RNA Preparation kit for Illumina (New England Biolabs) according the manufacture's protocol. For library size estimation we used the Bioanalyzer 2100. In cooperation with Prof. Dr. A. Grundhoff, head of the virus genomic research unit of the Heinrich-Pette-Institute Hamburg, we performed 50 cycles of cluster generation on cBot and further 50 bp single end sequencing on an Illumina HiSeq 2500. The sequencing output files were demultiplexed to fastq files using CASAVA software (version 1.8.2.). The data was checked on quality on Galaxy Platform (Goecks, et al., 2010; Giardine, et al., 2005; Blankenberg, et al., 2010) using the FastQC Tool (Babraham Bioinformatics, [Stand 04.02.2019, 14:35]) and the files were trimmed 11 bp from 5' end by using FASTQ Trimmer (Blankenberg, et al., 2010). Using TopHat Gapped-read mapper (Kim, et al., 2013), these trimmed fastq files were further mapped to human genome hg19. Therefore settings on Bowtie 2 were on 'very-sensitive' option. Next, Picard Tools SortSam (Picard Tools, [Stand 04.02.2019, 17:40]) on Galaxy was used to sort and coordinate the obtained bam files so that we could use them for read counting via HTSeq version 0.6.0 (Anders, et al., 2015) using following options: format (f) -> binary BAM files (bam), order (r) -> position (pos), stranded (s) -> no, minaqual (a) -> 10, feature type (t) -> exon and mode (m) -> union. After that, differential gene expression analysis was performed with the htseqcount files using DESeq2 (Love, et al., 2014) on Bioconductor version 3.2. The Wald test was used for one factor comparisons, whereas to test multiple terms at once the Likelihood ratio

test (reduced model) was used. The latter was used for differential analysis of conditions differing by more than one factor as well as for comparisons across all conditions and samples in the heatmap of Euclidian sample distances after regularized-logarithm (rlog) transformation and in principle component analysis (PCA) plot. For heatmaps with hierarchical clustering we used R programming tool 'gplots package heatmap.2' (Warnes, et al., [Stand: 04.02.2019, 15:33]). To reduce complexity and to perform enrichment analysis of gene sets, we did Gene Ontology analysis on R using the goseq package (Young, et al., 2010). From annotation data packages we used the 'org.Mm.eg.db' as well as the 'GO.db' library. The threshold values for regulated genes were set on: base mean (BM) >20, abs (log2fold change (L2FC)) >1, padj $\leq$ 0.5. For the GO analysis, all the pathways with FDR <0.001 were further used for visualization via bubble plots generated by 'Reduce + Visualize Gene Ontology' (REViGO) software (Suspek, et al., 2011) that clusters the related GO terms based on semantic similarity.

Results

UTX and JMJD3 knockdown alter factors of adipogenesis

Previously, H3K27me3 demethylases JMJD3 and UTX were discovered to play a role in MSC cell fate choice. It could be shown that JMJD3 and UTX inhibit the commitment of adipocyte and osteogenic lineage of MSCs (Ye, et al., 2012).

Firstly we wanted to reproduce these result. Therefore we used human mesenchymal stem cells, kindly provided from Prof. M. Kasem's lab in Odense, Denmark (Simonsen, et al., 2002). MSCs were immortalized by expression of telomerase reverse transcriptase (TERT), a catalytic subunit of the enzyme telomerase and passaged in different ratios (T4 1:4 ratio; T20 1:20 ratio). We performed siRNA mediated knockdown of JMJD3 and UTX in these cells which were then induced to differentiate into adipocytes. After 4 days of differentiation, we analyzed protein samples with Western blot as a knockdown efficiency control (Figure 2A). Interestingly an increase of UTX and JMJD3 level could be observed during adipocyte differentiation.

To assess the differentiation efficiency cells were stained with Oil Red O that allows to detect lipid droplets accumulation stained red. Interestingly, whereas the UTX knockdown resulted in increased stained lipid droplets compared to control cells both in T4 and T20 MSCs (Figures 2B and 2C), JMJD3 depletion did not show an effect on adipocyte differentiation in this experiment.

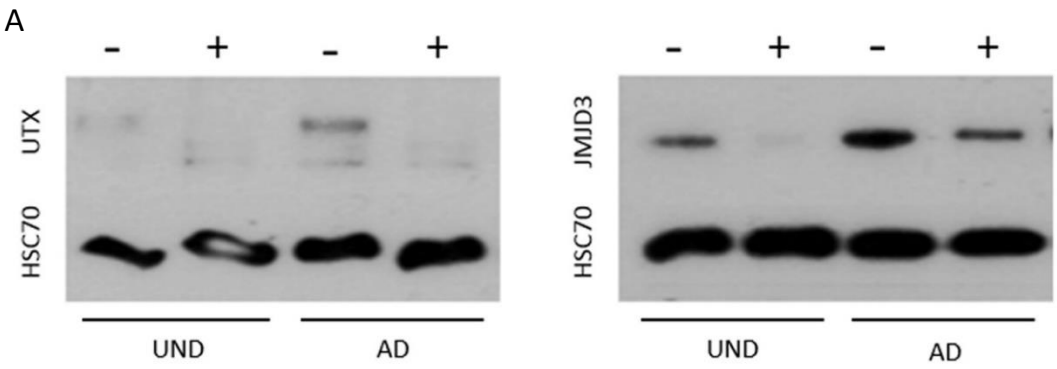

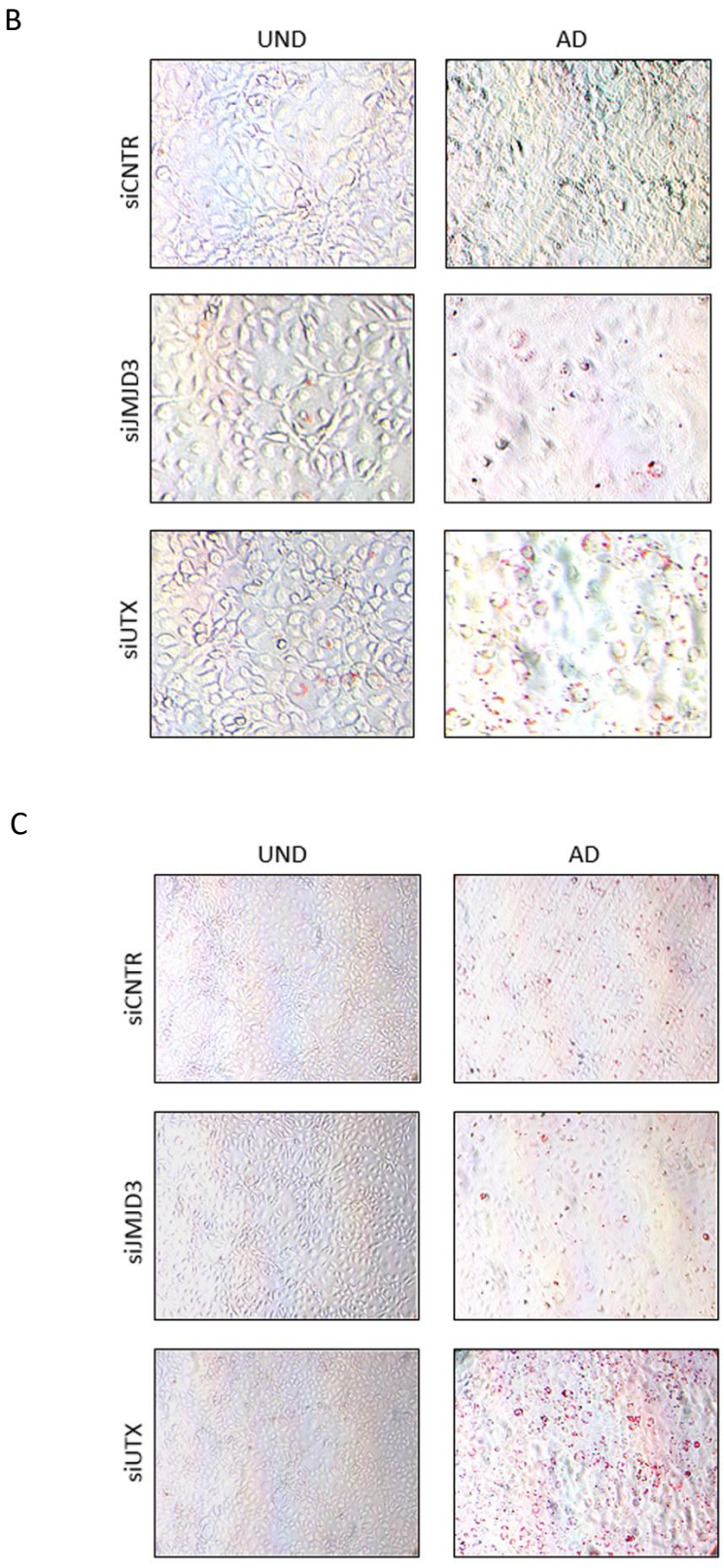

Figure 2. UTX knockdown enhances adipogenesis. (A) For a control of knockdown efficiency, MSCs T20 were transfected with UTX/JMJD3 siRNA (+) or Control siRNA (-) and differentiated into adipocytes or left undifferentiated. Protein samples were analyzed by Western blot with antibodies to UTX, JMJD3 and HSC70 (loading control). (**B)** Following Control, JMJD3 and UTX siRNA transfections, MSCs T4 and (**C**) T20 were induced to differentiate into adipocytes or left undifferentiated. Lipid droplet accumulation was visualized by Oil Red O staining after 4 days of differentiation.

To further explore alterations on gene expression, relative mRNA levels of several adipocyte-specific genes were analyzed by real-time PCR. Pyruvate dehydrogenase kinase isoenzyme 4 (PDK4) was upregulated upon UTX depletion in MSCs T4 (Figure 3C), supporting our previous observations in stainings. JMJD3 in this case did not show a significantly influence in PDK4 mRNA levels.

Whereas in other adipocyte-specific genes such as lipoprotein lipase (LPL) and dexamethasone-induced Ras-related protein 1 (RASD1) JMJD3 knockdown resulted in downregulation (Figure 3D-E). In these genes UTX knockdown led to a decrease of relative mRNA level as well. In contrast to western blot results gene expression of JMJD3 and UTX decrease during adipocyte differentiation in both cell lines.

Interestingly, in MSCs T20 PPARG and PDK4 as well as all other analyzed adipocyte-related genes, UTX and JMJD3 depletion led to a downregulation of gene expression (Figure 4C-F). Especially relative mRNA level of LPL, an early marker of adipocyte conversion, was reduced considerably upon JMJD3 knockdown (Figure 4E). The gene expression results in MSCs T20 go along with the presumption that depletion of the both H3K27me3 demethylases hampers adipocyte differentiation.

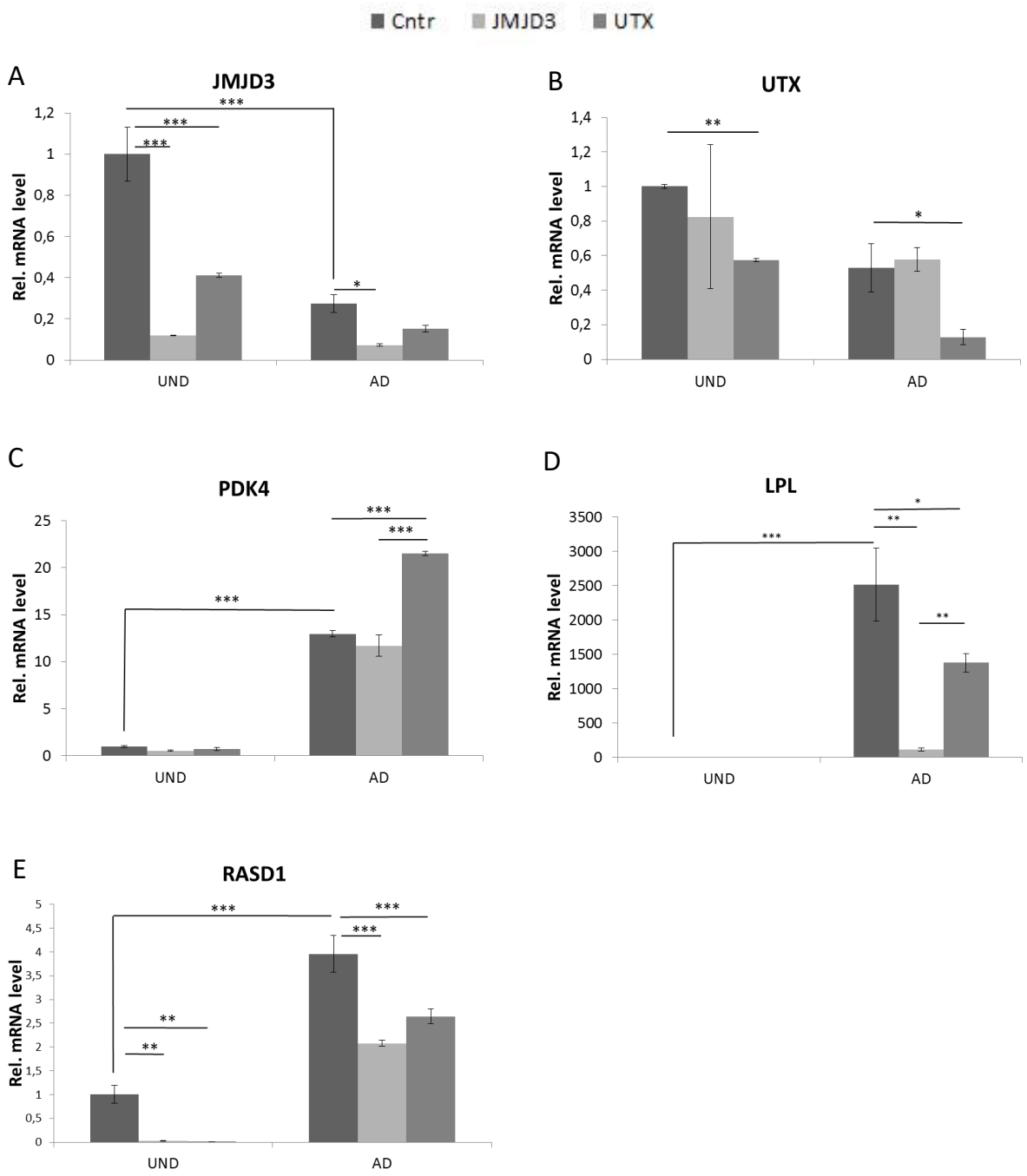

Figure 3. Expression of adipocyte-specific genes is altered upon JMJD3 and UTX knockdown in MSCs T4. Following Control, JMJD3 and UTX siRNA transfections, MSCs T4 were induced to differentiate for 4 days. Expression of genes were analyzed by real-time PCR with normalization to values of housekeeping gene HNRNPK. Efficiency of JMJD3 (**A)** and UTX (**B**) knockdown. (**C-E**) Relative gene expression of adipocyte marker genes. For statistical analysis Bonferroni's Multiple Comparison Test was performed where * $p<0.05$; ** $p<0.01$; *** $p<0.001$

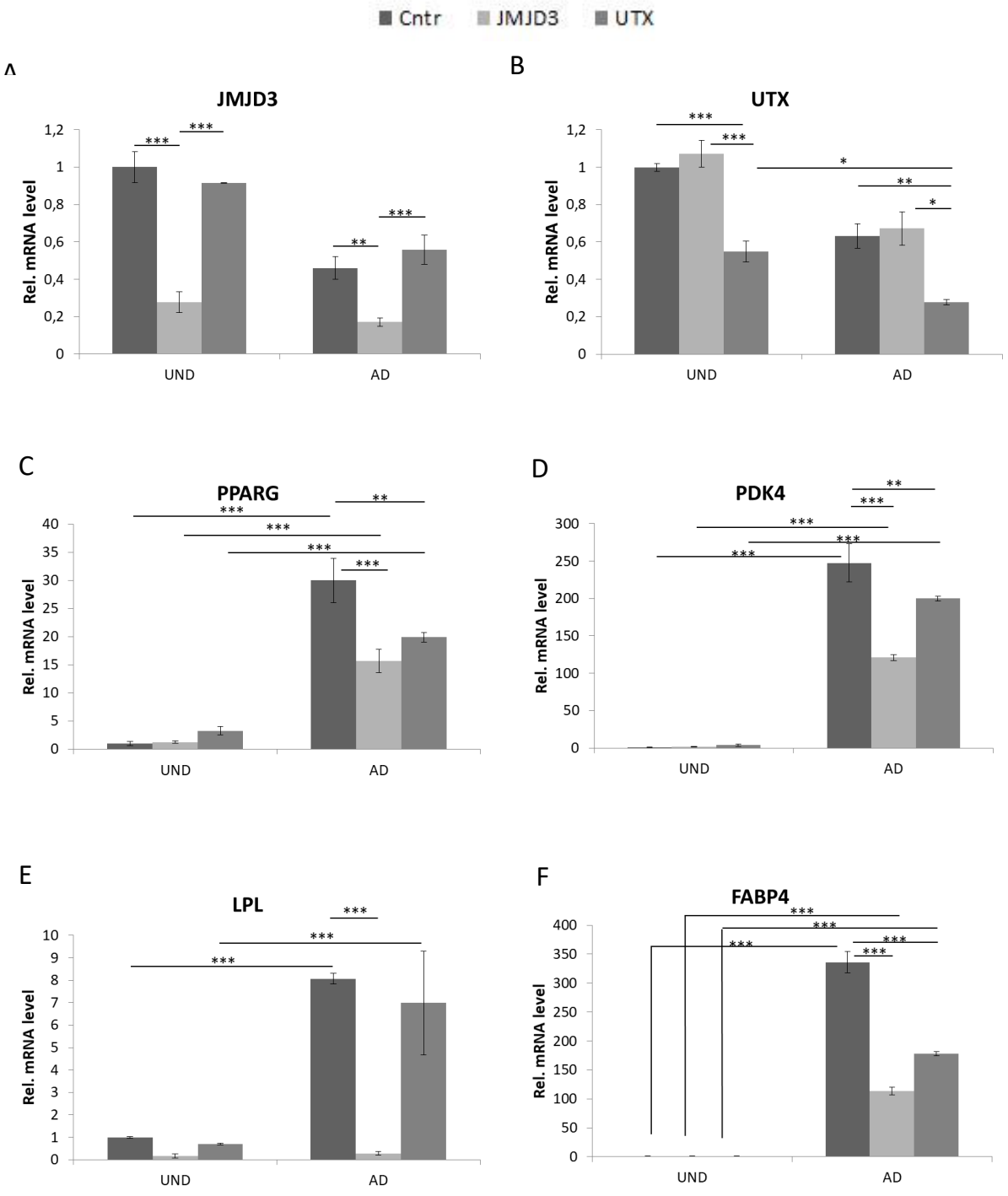

Figure 4. Expression of adipocyte-specific genes is decreased upon JMJD3 and UTX knockdown in MSCs T20. Following Control, JMJD3 and UTX siRNA transfections, MSCs T20 were induced to differentiate into adipocytes for 4 days. Expression of genes were analyzed by real-time PCR with normalization to values of housekeeping gene HNRNPK. Efficiency of JMJD3 (**A**) and UTX (**B**) knockdown. (**C-F**) Relative gene expression of adipocyte-specific genes. For statistical analysis Bonferroni's Multiple Comparison Test was performed where * $p<0.05$; ** $p<0.01$; *** $p<0.001$

JMJD3 knockdown promotes osteogenic differentiation in MSCs

Since depletion of JMJD3 and UTX lead to somewhat contradictory results in regulating adipocyte differentiation, we further investigated the importance of the H3K27me3 demethylases during osteogenic differentiation of MSCs. In a similar approach, MCSs were subjected to JMJD3 and UTX knockdown followed by 4 days of differentiation induction into osteoblast lineage. Knockdown efficiency control on protein level was done by Western blot. Once again JMJD3 an UTX protein levels were increased upon differentiation of MSCs into osteoblasts (Figure 5A).

As alkaline phosphatase activity is a marker for differentiating osteoblasts, we subsequently performed in vitro staining of MSCs that allows colorimetric detection of the alkaline phosphatase activity sites. Unexpectedly, we found that the knockdown of JMJD3 further enhanced the alkaline phosphatase activity predominantly in T4 (Figure 5B) and slightly in T20 MCSs (Figure 5C). The UTX depletion in MSCs T20 and T4 did not show significantly effects.

Consistently, gene expression studies confirmed staining results. Namely, the relative mRNA expression of osteoblast-lineage-specific genes alkaline phosphatase (ALPL), bone gamma-carboxyglutamate (Gla) protein (BGLAP) and RUNX2 was upregulated with JMJD3 knockdown in T20 MSCs. In contrast, UTX knockdown led to a significant reduced expression of the indicated genes (Figures 7C-E). Remarkably, relative mRNA level of RUNX2 was measured higher in undifferentiated JMJD3 depleted cells than in differentiated samples (7E).

Interestingly, the T4 MSCs revealed increase in ALPL induction upon JMJD3 knockdown consistent with the results in T20 MSCs, whereas the BGLAP was significantly downregulated in these cells (Figure 6C and D). UTX depletion led to significantly lower levels of BGLAP expression, too (6D).

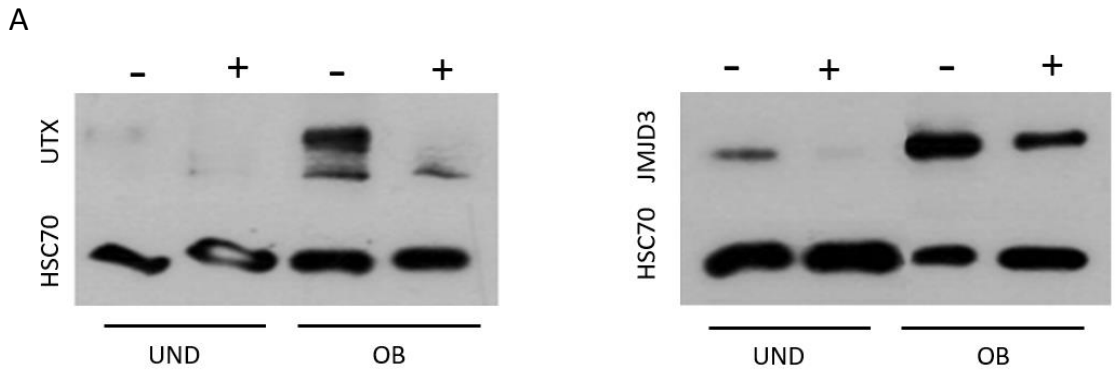

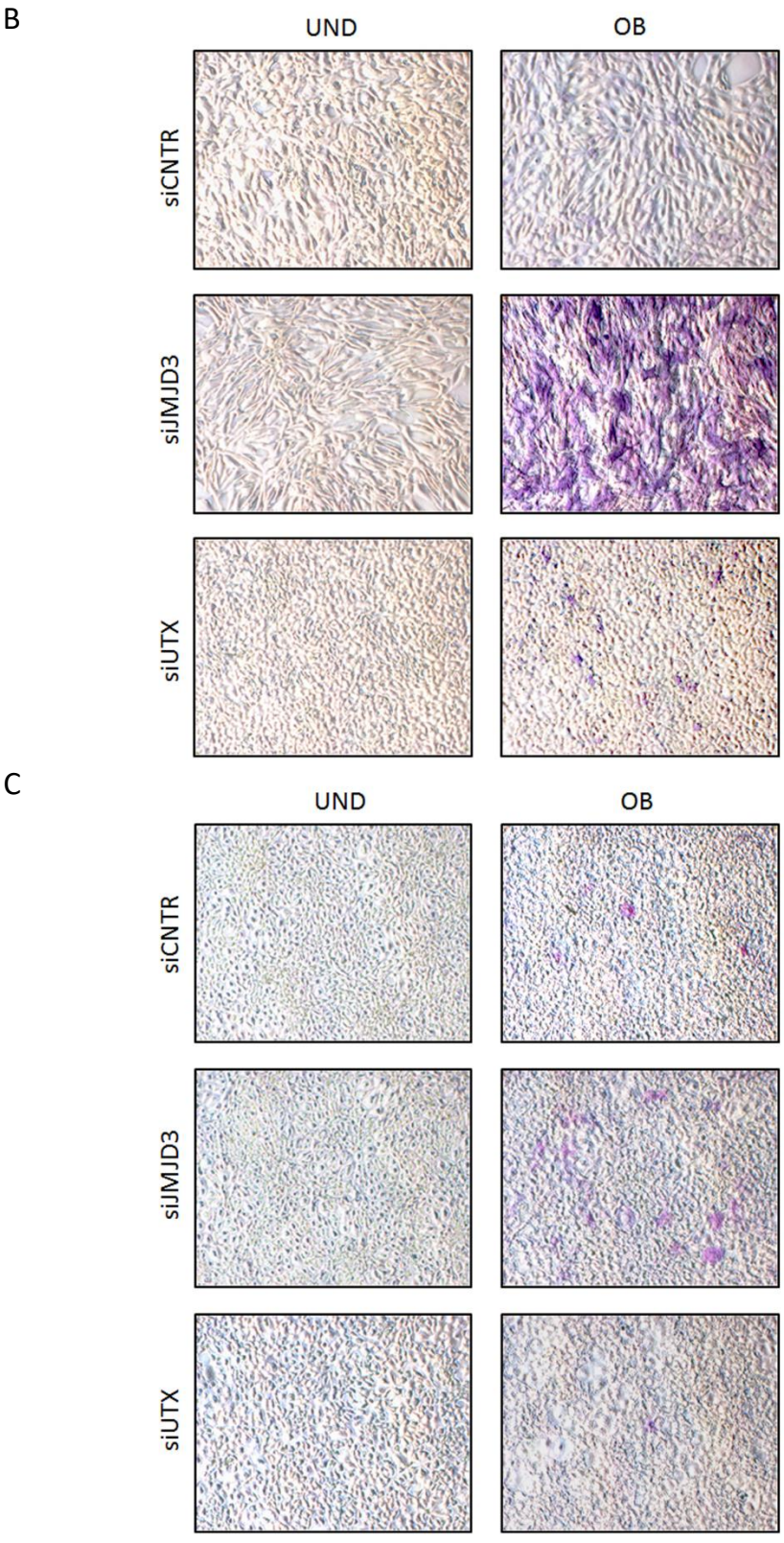

Figure 5. JMJD3 depletion increases osteoblast differentiation. To check knockdown efficiency on protein level, MSCs T20 were transfected with UTX/JMJD3 siRNA (+) or Control siRNA (-) and differentiated into osteoblasts or left undifferentiated. Protein samples were analyzed by Western blot with antibodies to UTX, JMJD3 and HSC70 (loading control) (**A**). Following Control, JMJD3 and UTX siRNA transfections, MSCs T4 (**B**) and T20 (**C**) were induced to differentiate into osteoblasts or left undifferentiated for 4 days. Alkaline Phosphotase staining was used to visualize osteoblast differentiation**.**

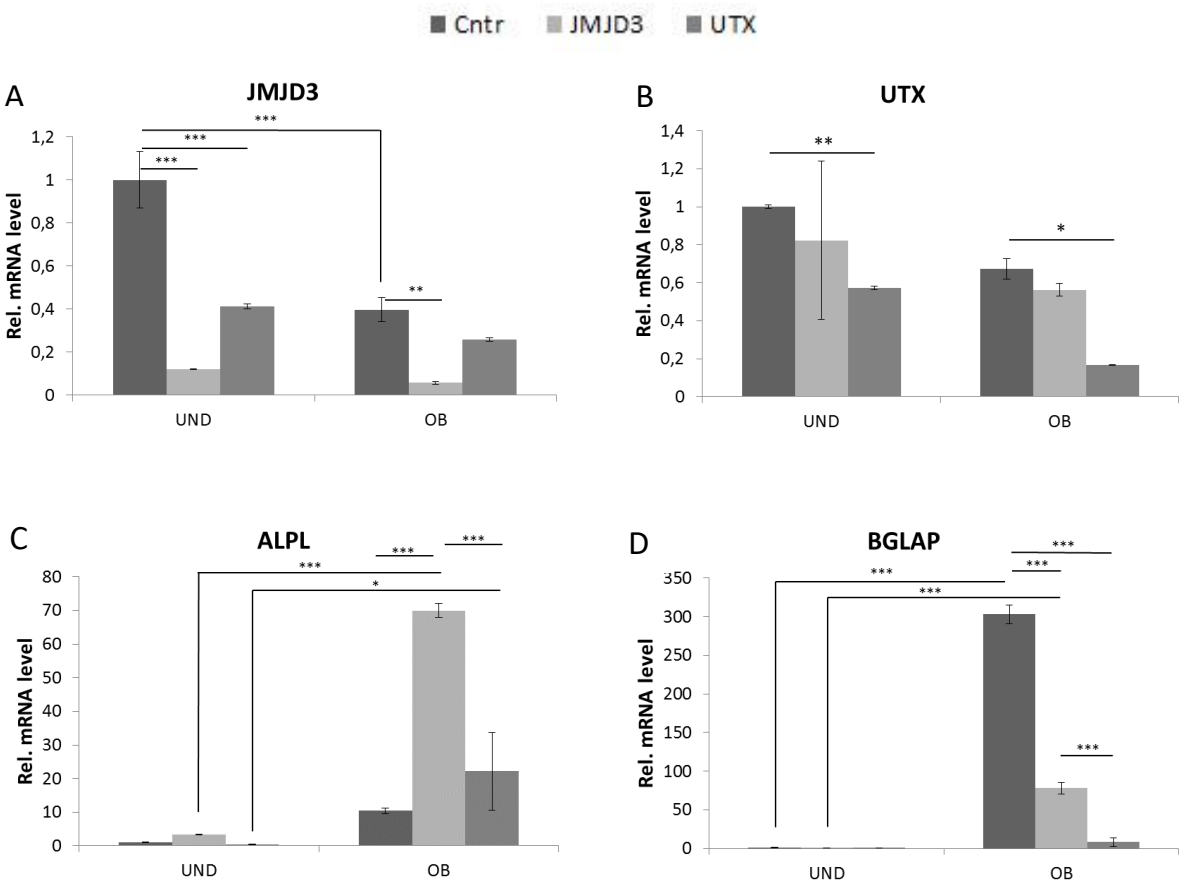

Figure 6. Expression of osteoblast marker genes is altered upon JMJD3 and UTX knockdown in MSCs T4. Gene expression was analyzed by real-time PCR with normalization to values of housekeeping gene HNRNPK. Efficiency of JMJD3 (**A**) and UTX (**B**) knockdown. Relative gene expression of alkaline phosphatase (**C**) and BGLAP (**D**). For statistical analysis Bonferroni's Multiple Comparison Test was performed where* $p<0.05$; ** $p<0.01$; *** $p<0.001$

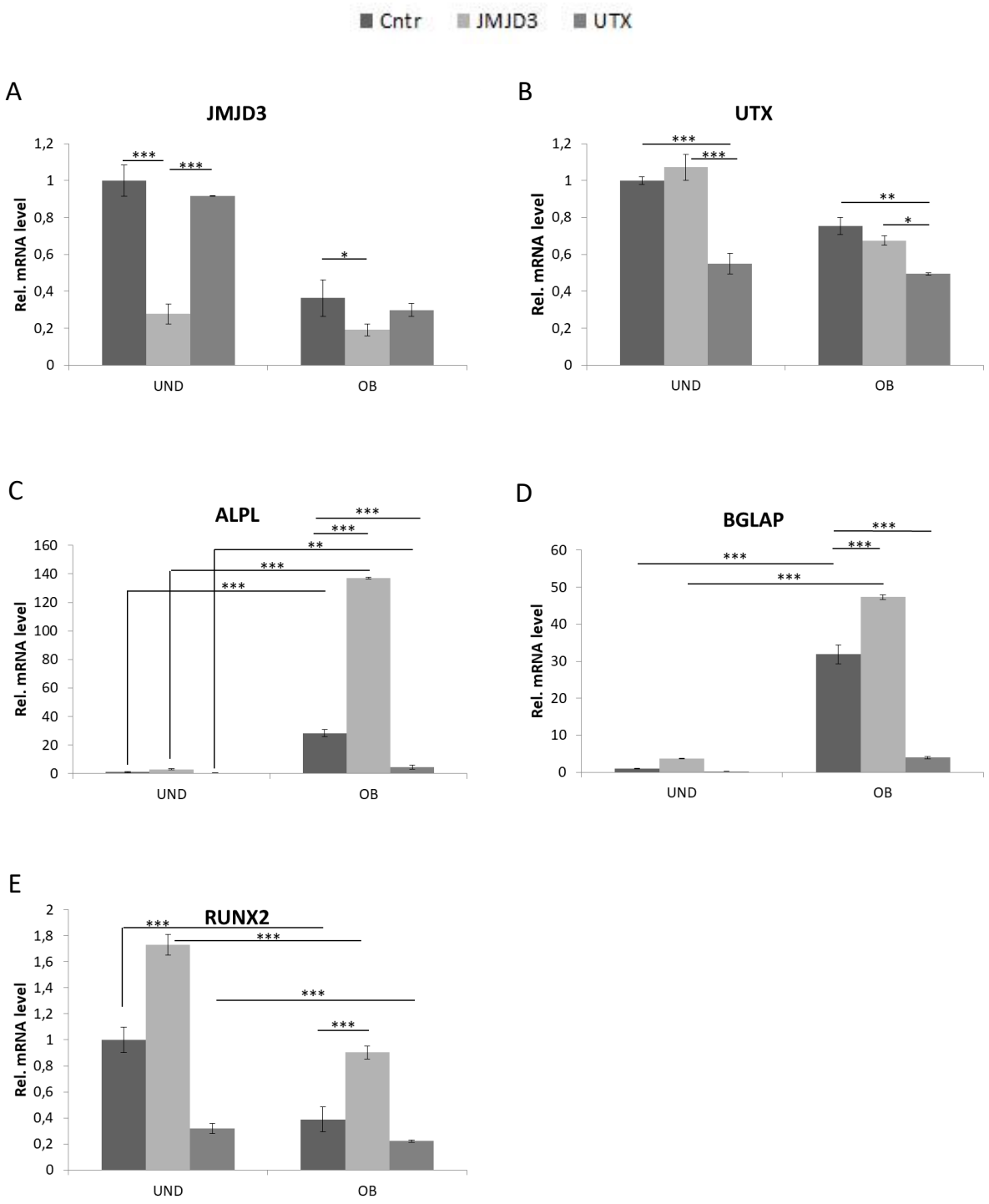

Figure 7. Expression of osteoblast-specific genes is increased upon JMJD3 knockdown in MSCs T20. Expression of genes were analyzed by real-time PCR with normalization to values of housekeeping gene HNRNPK. Efficiency of JMJD3 (**A**) and UTX (**B**) knockdown. Relative mRNA levels of osteoblast-specific genes (**C**-**E**). For statistical analysis Bonferroni's Multiple Comparison Test was performed where * $p<0.05$; ** $p<0.01$; *** $p<0.001$

JMJD3/UTX inhibition by GSK-J4 promotes osteoblast-specific gene expression

GSK-J4 is a specific small-molecule inhibitor for H3K27me3 demethylases JMJD3 and UTX, allowing pharmalogical intervention across the jumonji enzymes. It is a prodrug which gets activated by macrophage esterases to GSK-J1. GSK-J1 works as a competitive inhibitor of α-ketoglutarate and Fe^{2+}, two cofactors dependent for enzymatic activity of demethylases JMJD3 and UTX (Kruidenier, et al., 2012).

To investigate if the inhibitor shows similar effect on MSC differentiation like knockdown of JMJD3/UTX especially towards osteoblast lineage, MSCs T20 following osteoblast differentiation were treated with 1µM of GSK-J4.

As a positive control we performed Western blot analysis. H3K27me3 protein level increases upon GSK-J4 treatment in both conditions (Figure 8A). Analysis of osteoblast-marker genes ALPL, BGLAP and G6PD showed the tendency that treatment with GSK-J4 leads to increased mRNA levels of these genes, although the difference in ALPL and G6PD is not statistical relevant (8B-D).

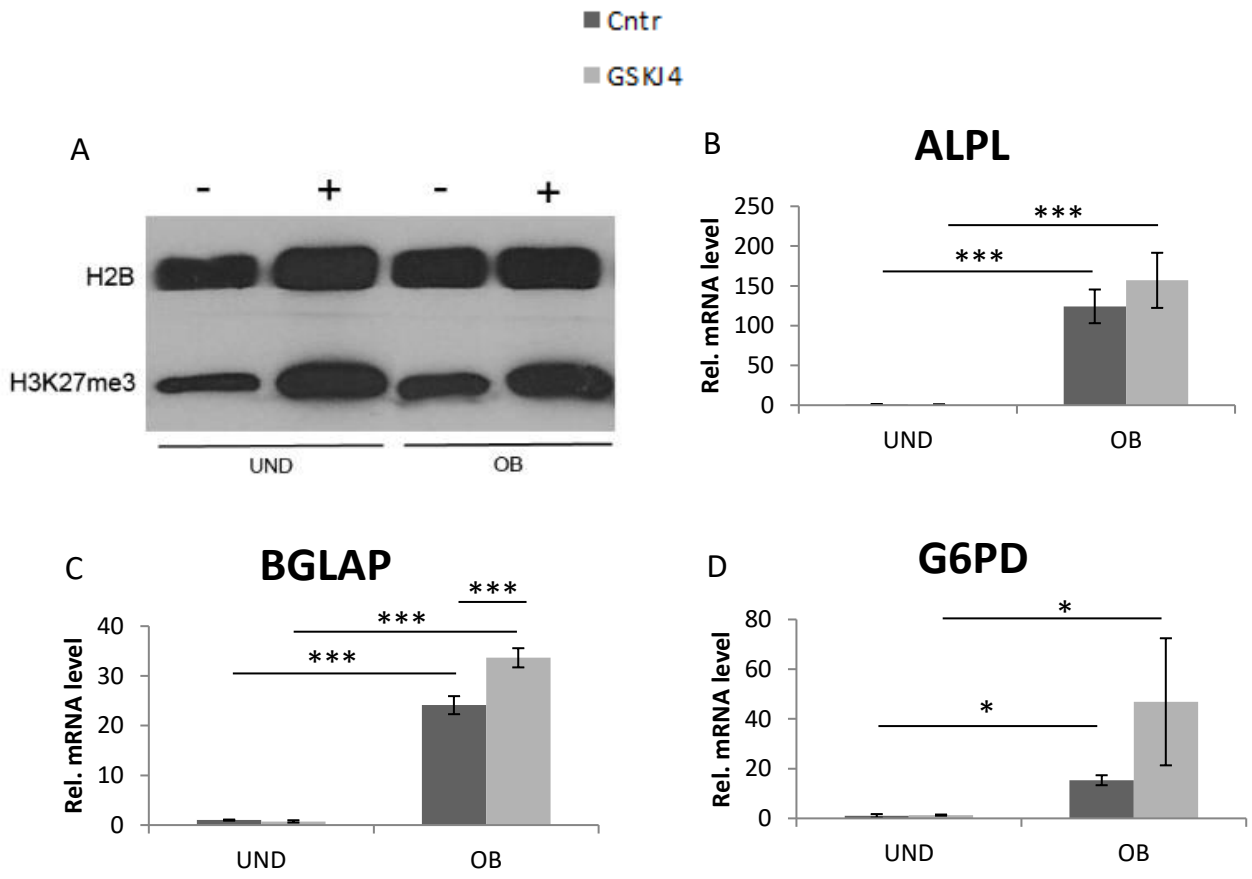

Figure 8. GSK-J4 treatment increases osteoblast differentiation. MSCs T20 were treated with ethanol (Cntr) or GSK-J4 for 5 days of differentiation. **(A)** To check inhibition efficiency protein samples either treated with GSK-J4 (+) or ethanol (-) were analyzed by Western blot with antibodies to H3K27me3 and H2B (loading control). **(B-D)** Relative mRNA levels of osteoblast-specific genes. For statistical analysis Bonferroni's Multiple Comparison Test was performed where * p<0.05; ** p<0.01; *** p<0.001

Transcriptome profiling reveals condition specific gene expression patterns

In order to get an overall picture of the role of JMJD3 during differentiation we performed transcriptome wide analysis of gene expression changes induced by JMJD3 knockdown in MSCs. Interestingly, as revealed by principal component analysis, the differentiation induced changes (along the PC1 component) in MSCs were in general maintained in knockdown conditions in each state, respectively (Figure 9A). The similar pattern was observed for JMJD3 knockdown induced variations between the each state of MSCs (along the PC2 component). Importantly, the clustering analysis further supported the similarity of the replicates of each state and condition and moreover revealed the clustering of control and JMJD3 siRNA treated conditions within the each state. To visualize sample-to-sample distances, we used principal-components analysis (PCA) (Figure 9A) and Euclidean heatmap (Figure 9B). The PCA Plot shows that the replicates of each condition lie close to each other implicating a high similarity (each circle represents one individual sample). Furthermore, the differences and directions from undifferentiated samples to differentiated samples among the control group is similar to the difference of undifferentiated samples to differentiated samples treated by siJMJD3. For example comparing undifferentiated control to osteoblast control reveals a similar direction and distance than undifferentiated and osteoblast samples with JMJD3 knockdown, meaning that differentiation induced changes are similar between them. Further we observed that JMJD3 depletion induced similar changes between the samples in each condition (e.g. undifferentiated Control to undifferentiated siJMJD3).

Another way to test and visualize how the samples are connected to each other is the Euclidean heatmap. To create it, we used data after rlog transformation to avoid that some highly variable genes dominate the distance measurement. Samples were independently and hierarchically clustered by the Euclidean distance. We again assessed, that each pair of replicates cluster together. Moreover, we found that all JMJD3 knockdown samples lie close to their respective controls. Both methods of visualizations showed us that RNA-seq derived transcriptomes are characteristic to the different conditions.

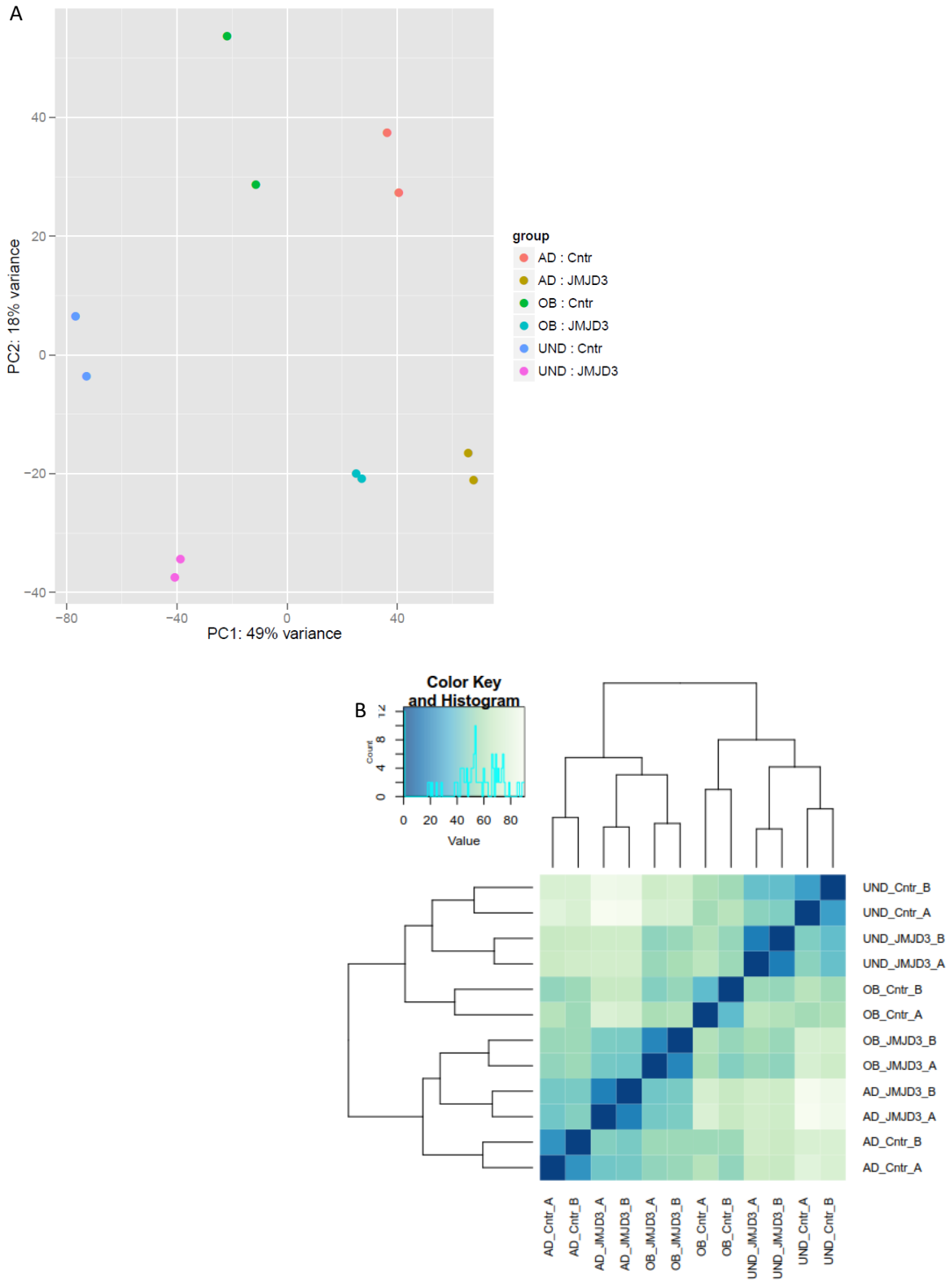

Figure 9. Overall gene expression similarity of the samples in a PCA Plot and Euclidean heatmap. Principle component analysis (PCA) Plot (**A**) and heatmap of Euclidean sample distances after rlog transformation (**B**) were compiled as a quality control to evaluate overall similarity between the samples.

To further investigate the differences in gene expression induced with differentiation and JMJD3 knockdown, we created a heatmap depicting the Z-score values of rlog transformed counts of the top 500 genes that showed highest variance across the samples (Figure 10A). The hierarchical clustering of gene expression changes in each condition further revealed that adipocyte and osteoblast differentiation resulted in differential regulation of genes as compared to undifferentiated control. Moreover, the overall picture of gene expression upon JMJD3 loss during differentiation suggested that whereas some clusters of genes were not affected by JMJD3 knockdown, the rest were regulated in a differential manner either blocked or further enhanced following JMJD3 depletion in each state, respectively. Interestingly the same pattern was observed for JMJD3 knockdown induced changes in undifferentiated state. In general, there were some genes which were up- and downregulated in all the conditions independent of the differentiation status.

Next we checked for the overlap of genes that were down- and up regulated upon JMJD3 knockdown compared to respective controls. Therefore we created Venn diagrams depicting the number of overlapping genes that were up- or downregulated in the several conditions (Figures 10B and 10C).

Venn diagram of genes that were downregulated upon JMJD3 depletion reveals that 207 in undifferentiated state, 170 genes in adipocytes and 237 genes in osteoblasts were downregulated in this condition exclusively. Moreover, the number of genes that overlap in the differentiated state (between adipocytes and osteoblast) was with 184 distinctly higher than the overlap between each differentiated state with undifferentiated condition (Figure 10B).

Regarding genes that were upregulated upon JMJD3 depletion, Venn diagram shows with 503 a high number of genes expressed exclusively in undifferentiated MSCs. Still there are 278 genes in osteoblasts and 144 genes in adipocytes upregulated, solely. Furthermore, there is a higher overlap of 197 genes between undifferentiated cells and osteoblasts compared to 53 genes overlapping between undifferentiated and adipocyte condition. Taken together, the different conditions base on distinct gene expression patterns influenced by JMJD3 depletion.

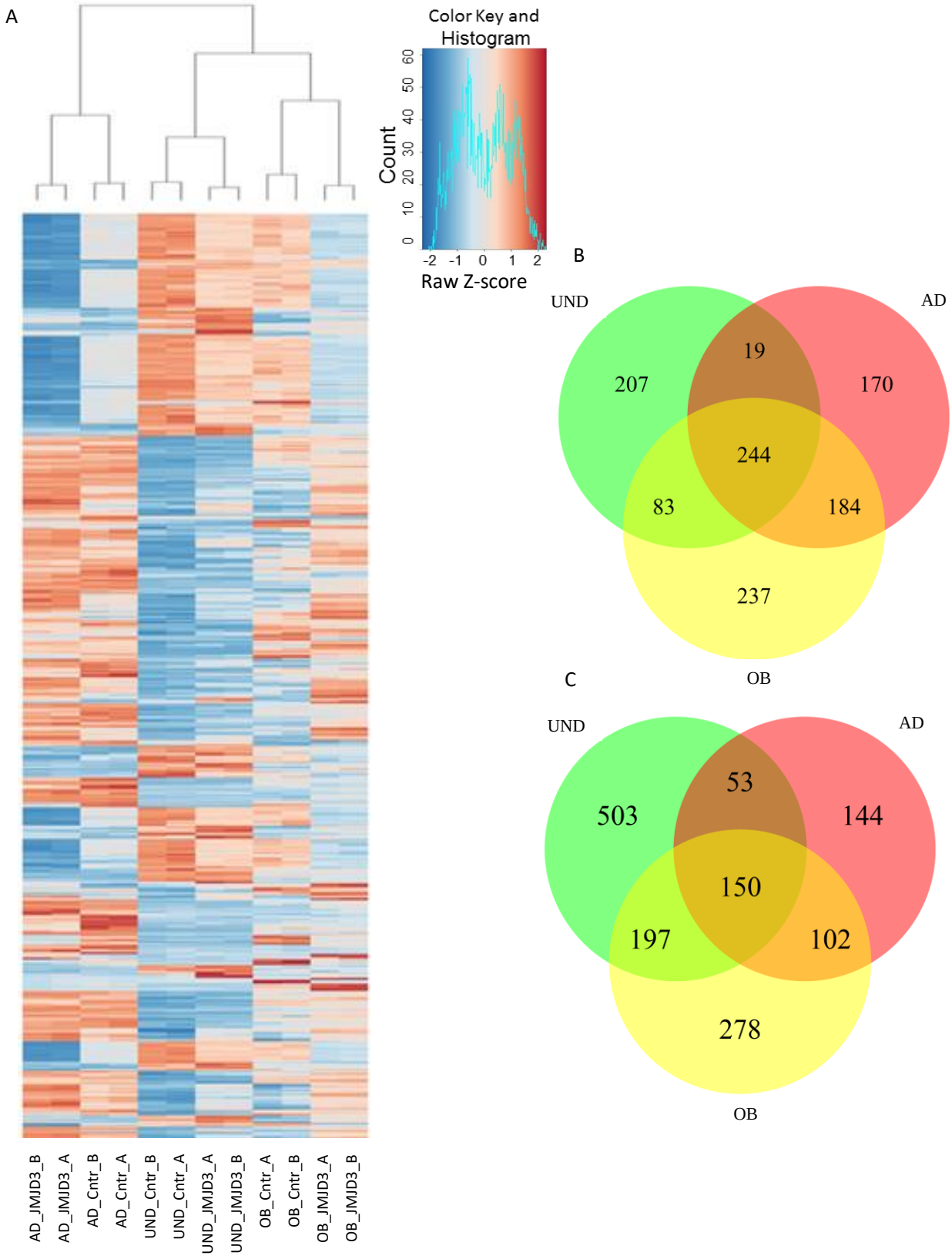

Figure 10. (**A**) Heatmap depicting the Z-score values of the regularized-logarithm (rlog) transformed counts of the top 500 genes that show highest variation across all samples with the hierarchical clustering of replicates. (The colour key and histogram shows the number of counts and the raw Z-score. Colored in blue is the negative Z-score, implying that the gene expression for this special gene in the given condition was lesser than the overall mean gene expression of all the samples together. The opposite is true for red colored positive raw z-score.) Venn diagrams show the overlaps in the siJMJD3 downregulated (**B**) and upregulated genes (**C**) in each differentiation condition, respectively.

JMJD3 knockdown negatively influences gene expression related to cell division but promotes tissue development in undifferentiated and differentiated MSCs

We then asked which genes were up- or downregulated upon JMJD3 knockdown in each condition compared to respective control. Therefore, we did Gene Ontology (GO) pathway analysis. The resulting data was summarized and clustered by REViGO software, with which long lists of GO data can be visulaized. We created semantic similarity-based scatterplots out of preselected different gene functional categories related to MSC differentiation, chromosomal and general cell aspects to prioritize project relevant gene clusters.

Surprisingly, genes downregulated upon JMJD3 knockdown were highly enriched in pathways associated with cell division such as cell cycle, nuclear division, mitotic cell cycle and DNA replication (Figures 11A, 12A and 13A). This indicates that normal levels of H3K27me3 are important for proper cell cycle regulation and division. Interestingly, the genes upregulated upon loss of JMJD3 were already in undifferentiated state associated with pathways relevant for bone formation and phenotype such as extracellular matrix, ossification and tissue development (Figure 11B). Given the fact that bone marrow derived MSCs are more osteoblast predisposed than adipocyte, this further suggests that loss of JMJD3 is essential for maintaining the differentiation choice of MSCs along the osteoblastic lineage. This was consistently apparent in osteoblast state as well following the JMDJ3 depletion (Figure 13B). Interestingly, the genes upregulated in adipocyte state upon JMJD3 knockdown were mainly associated with cell death and apoptosis which could explain why the cells failed to become functional adipocytes once JMJD3 was lost. Altogether, these findings suggest that JMDJ3 more or less targets the similar sets of genes involved in cell cycle regulation independent of differentiation status. Notably, the substantial differences in phenotypes among the three states of MSCs analyzed in this study come most likely through indirect mechanisms of gene expression regulation induced upon JMJD3 loss (the upregulated genes).

Regarding now gene clusters that were upregulated in all three conditions, it is in evidence that locomotion and tissue development are upregulated upon JMJD3 depletion (Figures 11B, 12B and 13B). Cell locomotion is the ability of a cell to create movement and thus it is important for cell migration. Our data indicates that knockdown of JMJD3 and as a result a high H3K27me3 level results in increased cellular locomotion and thus facilitates cell migration and homing. Interestingly, transcription of genes related to tissue development was significantly increased. That leads to the idea that JMJD3 prevents general tissue development which concurs with our observations of increased osteoblast differentiation upon JMJD3 depletion.

JMJD3 knockdown promotes tissue development and ossification related gene expression in undifferentiated MSCs

We proceeded our analysis of sequencing data looking at the gene expression clusters of each condition separately. In undifferentiated MSCs, genes related to mitotic cell cycle are highly significantly downregulated upon JMJD3 depletion. Moreover chromosomal segregation and chromatin remodeling at the centromere are decreased indicating the influence of JMJD3 to chromosomal distribution and proper cell division during mitosis and meiosis. Together with a decreased DNA replication, nucleic acid metabolism related genes are downregulated. This data reveals that JMJD3 might be an important player in promoting proliferation and growth processes (Figure 11A).

It is known that PcG proteins influence different aspects of DNA damage response by regulating specific cell cycle checkpoints (Wu, et al., 2011) or by affecting double-strand break repair (Chang, et al., 2011). Here we could demonstrate that JMJD3 plays a role in regulation of gene expression related to DNA damage, as the cell response to DNA damage cluster, which includes DNA repair mechanisms is downregulated upon JMJD3 knockdown (Figure 11A).

Regarding the scatterplot of gene clusters that were upregulated in undifferentiated MSCs we interestingly found that beneath cell proliferation and its regulation, ossification cluster showed up. It seems that JMJD3 knockdown itself can lead to an increase of ossification related genes, though no differentiation factors are substituted. As a reverse conclusion we could assume that the H3K27me3 demethylase JMJD3 hampers ossification already in an undifferentiated state of MSCs (Figure 11B).

It was shown by previous work done by De Santa et al. that JMJD3 is linked to inflammation. It was found to be expressed in macrophages in response to inflammatory cytokines and bacterial products (De Santa, et al., 2007). Moreover we discovered that genes related to immune system process were upregulated upon JMJD3 depletion in undifferentiated MSCs (Figure 11B).

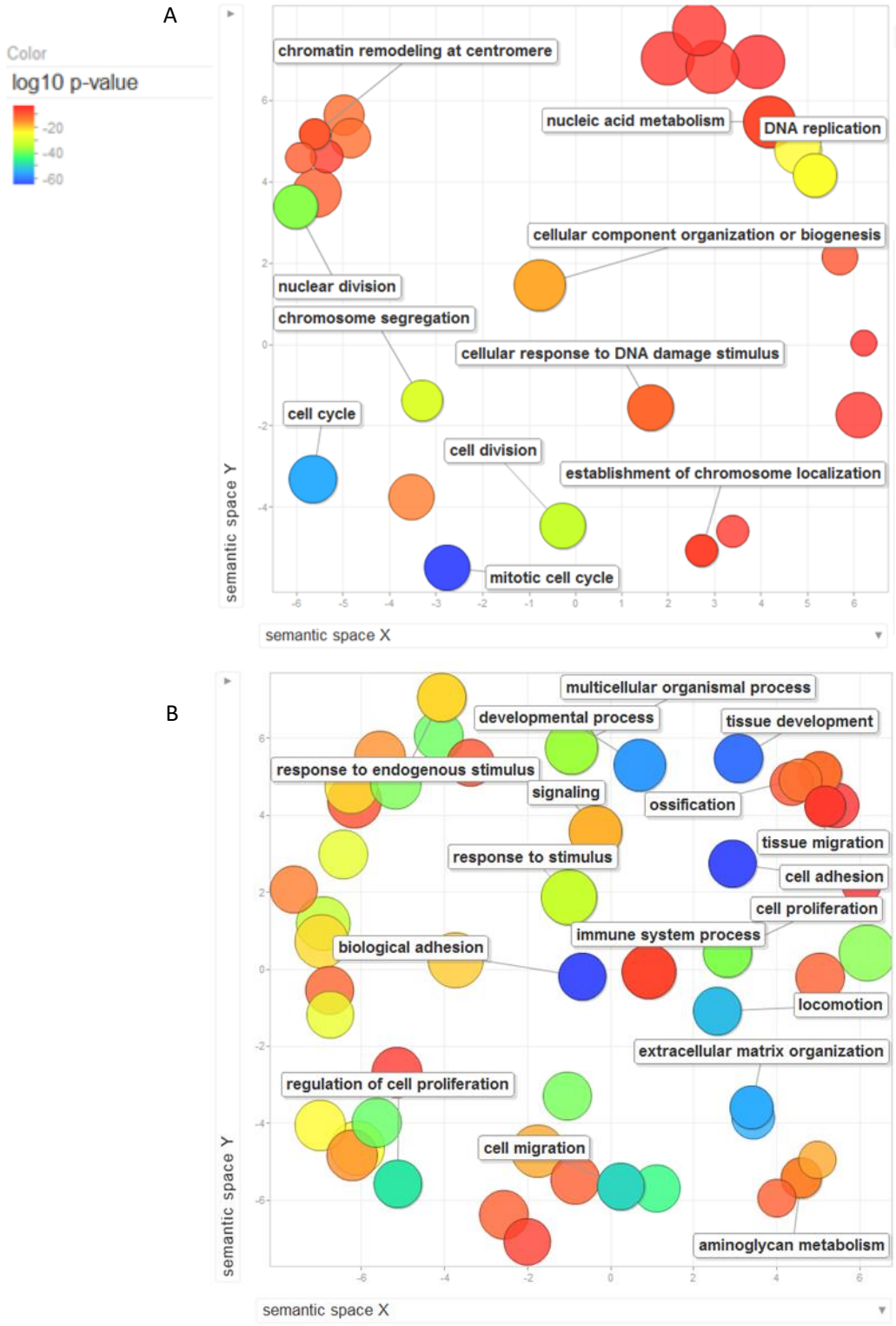

Figure 11. Gene Ontology (GO.BP) pathway analysis of undifferentiated cell samples. Scatterplots depict the cluster representatives of JMJD3 regulated genes in undifferentiated condition. Bubble colors indicate the log10 p-value; size of the bubbles describe the frequency of the GO term in the database (are bubbles are of more general terms). (**A**) Scatterplot of genes that are downregulated upon JMJD3 knockdown compared to control. (**B**) siJMJD3 upregulated genes in comparison to control, respectively.

JMJD3 depletion leads to upregulation of genes participating in apoptosis and p53 signaling transduction

Scatterplots of Gene Ontology pathway analysis of adipocyte samples revealed that JMJD3 knockdown leads to increased expression of genes that are involved in cell death and regulation of apoptotic process as well as in apoptotic cell clearance (Figure 12B). If we hypothesized that JMJD3 overexpression would result in antagonistic effect, it could be an interesting tool in investigation and research about ageing.

Beneath upregulation of cell death and apoptotic cell clearance, signaling transduction of p53 was increased in adipocytes as well (Figure 12B).

Among the cluster representatives of JMJD3 knockdown downregulated genes in adipocytes were again cell division related clusters like chromosome segregation and cellular component organization and biogenesis. Moreover cell proliferation and reproduction related gene expression was decreased (Figure 12A). Overall it shows a similar pattern compared to scatterplots depicting downregulated clusters in undifferentiated MSCs and in osteoblast (Figures 11A and 13A). This indicates that fundamental alterations among the three conditions happen particularly in upregulation of specific genes.

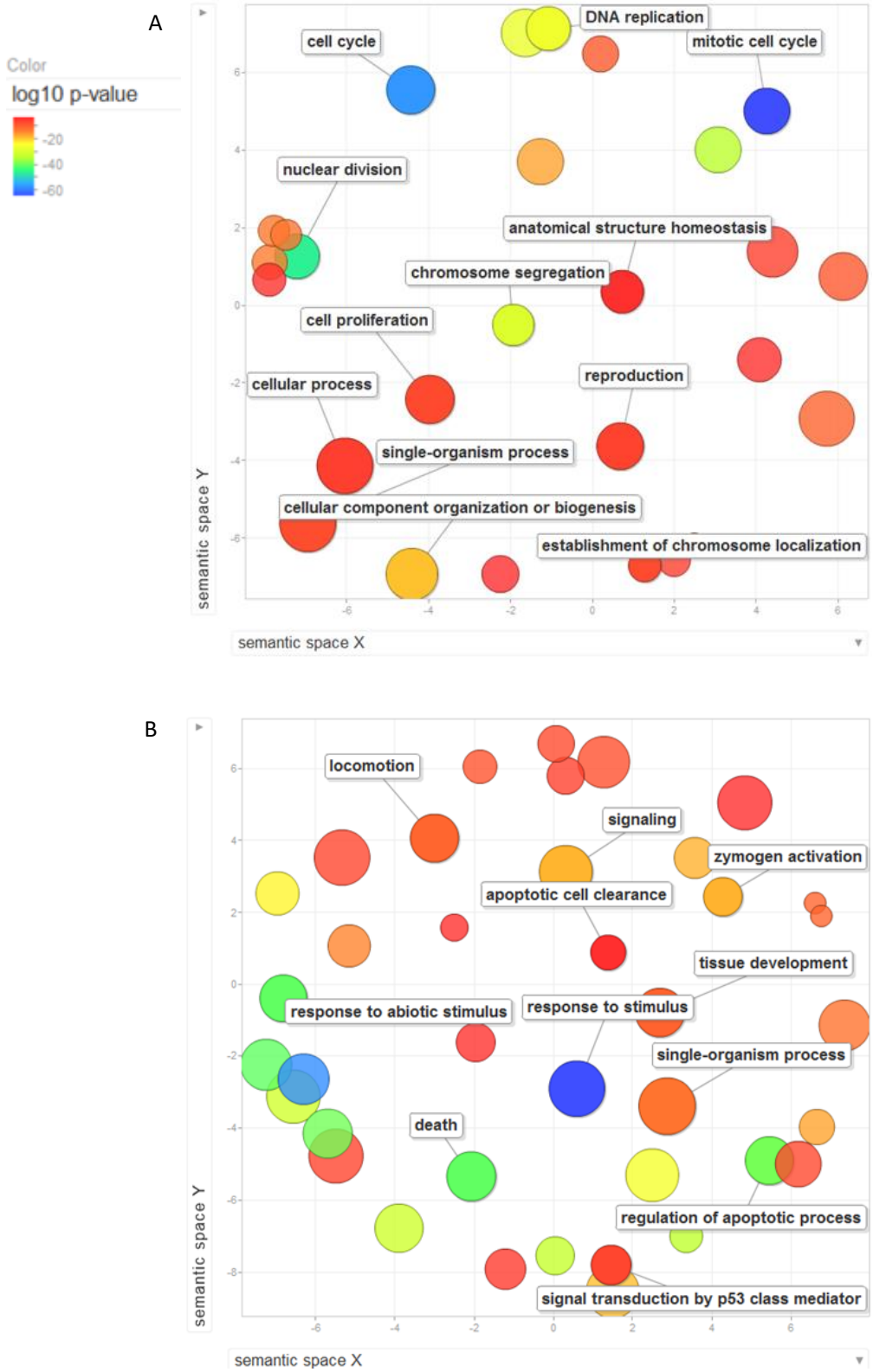

Figure 12. Gene Ontology (GO.BP) pathway analysis of adipocyte samples. Scatterplots depict the cluster representatives of JMJD3 regulated genes in adipocytes. Bubble colors indicate the log10 p-value; size of the bubbles describe the frequency of the GO term in the database. (**A**) Scatterplot of genes that are downregulated upon JMJD3 knockdown compared to adipocyte control. (**B**) Scatterplot of genes upregulated upon JMJD3 depletion.

Ossification related genes are upregulated upon JMJD3 knockdown

Regarding scatterplots of osteoblast samples reveals that ossification is increased upon JMJD3 knockdown, supporting our observations in stainings and PCR experiments before. Beneath ossification, lipid and collagen metabolism are upregulated as well, indicating the importance JMDJD3 has in several metabolic processes. Beside regulation of metabolic genes, JMJD3 knockdown promotes tissue development and positive regulation of developmental process as well as positive regulation of biological process (Figure 13B). All in all we see that JMJD3 plays an essential role in biological fields that all imply growth and tissue development and maintenance.

Compared to scatterplots of downregulated genes in undifferentiated and adipocyte condition, we see regarding osteoblast samples a similar pattern of clusters. Cell division and reproduction related genes are downregulated, just like cell proliferation and DNA replication. Taken together, by demethylation of H3K27me3 and removing the repressive marks from distinct genes, JMJD3 is needed for process of cell growth and division.

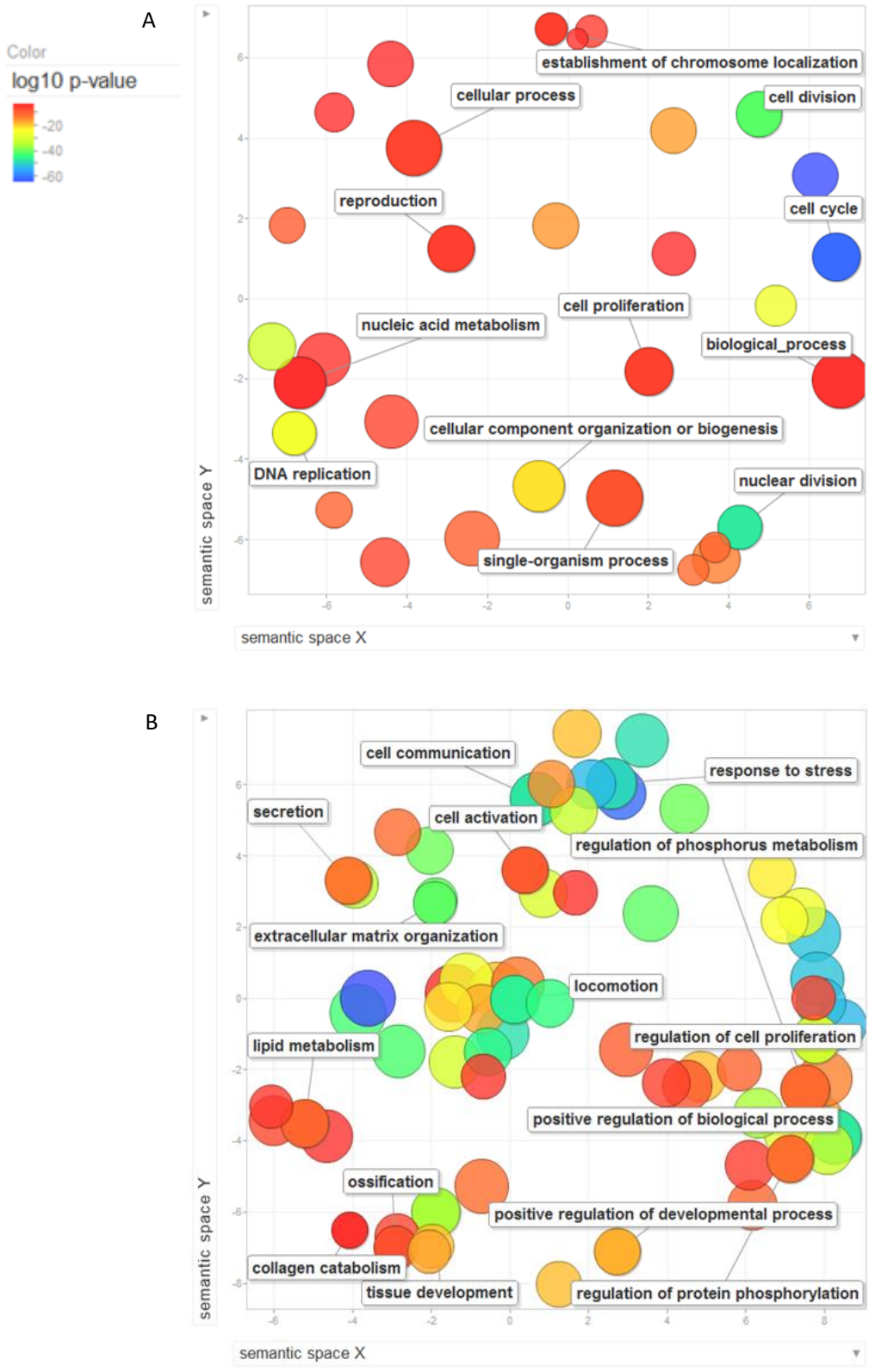

Figure 13. Gene Ontology (GO.BP) pathway analysis of osteoblast samples. Scatterplots show the cluster representatives of JMJD3 regulated genes in osteoblasts. Bubble colors indicate the log10 p-value; size of the bubbles describe the frequency of the GO term in the database. (**A**) Scatterplot of genes that are downregulated upon JMJD3 knockdown compared osteoblast control. (**B**) Scatterplot of genes upregulated upon JMJD3 depletion.

Discussion

It is well known that development of cell phenotype is tightly controlled by transcription factors, nevertheless the role of epigenetic regulation due to post-translational histone modifications remains in broad areas unknown. Histone modifications are involved in many cellular processes, regulating chromatin accessibility and gene activation or inhibition. Previous studies done by the our group demonstrated that dynamic changes in post-translational histone modifications are essential for the differentiation of multipotent human mesenchymal stem cells to the adipocyte and osteoblast lineage (Karpiuk et al., 2012). Moreover it had been demonstrated that some adipocyte-specific genes exist in a bivalent epigenetic state, carrying both activating H3K4me3 and repressive H3K27me3 marks. It was shown that upon differentiation, these genes exhibit a loss of the repressive mark, while H3K4me3 mark remains unchanged. The resolution of the bivalency in this case was shown to be dependent on RNF40 mediated monoubiquitination of target genes. In this study we further deciphered the importance of H3K27me3 demethylation by two histone demethylases JMJD3 and UTX in regulating the lineage commitment of hMSCs into adipocytes or osteoblasts.

It is essential for a better understanding and treatment of osteopathologies, to investigate the regulatory mechanisms controlling the lineage commitment of hMCSs. During osteoporosis, a common disease in ageing population, bone loss is associated with a conversion of bone in favor to disassembling osteoclasts. Furthermore, insufficient osteoblastogenesis due to an imbalance of adipogenesis and osteoblastogenesis leads to increased bone fragility and increased danger of fractures as reviewed from (Pino, et al., 2012). However, a mechanism that leads to the switch from osteoblast to adipocyte differentiation in ageing cells is not yet discovered.

According to our findings, JMJD3 and UTX depletion decreased the expression of adipocyte-specific genes that were tested. While lipid droplet formation in Oil Red O staining was slightly enhanced upon UTX knockdown, gene expression studies showed mostly the contradictory results. Interestingly, the two types of hMSCs used in this study showed clear differences in gene expression change of adipocyte marker genes upon JMJD3 knockdown. While the expression of PDK4 was increased in MSCs T4 upon UTX knockdown this gene was downregulated in the equally designed experiment in MSCs T20. Based on the estimated decrease of additional adipocyte-specific genes LPL, RASD1 and FABP4 upon JMJD3 and UTX depletion, we could strengthen our hypothesis, that active demethylation of H3K27me3 is essential for MSC differentiation towards adipocyte lineage.

Differences between hMSCs T4 and T20 have been described before from Serakincic et al. (Serakinci, et al., 2004), who discovered that hMSCs T20 and T4 exhibit a loss of contact inhibition at different population doubling levels (PDL). Additionally, T20 MSCs showed anchorage independence and formed tumors in mice unlike T4 MSCs. Furthermore, in hMSCs T20 expression of cell-cycle associated gene DBCCR1 was lost due to hypermethylation of its promoter, correlating with first detection of tumor formation in immune-deficient mice whereas T4 MSCs acquired at later PDL an activating mutation of KRAS (Serakinci, et al.,

2004). These data reveals that hMSCs T4 and T20 have different properties and change genetically, epigenetically and phenotypically during population doubling process.

To our surprise we discovered osteoblast inhibitory function of JMJD3 where its loss consistently resulted in increased Alkaline Phosphotase staining and osteoblast-specific gene expression in both MSCs T4 and T20. In contrast, UTX knockdown did not exhibit the same effect in these cells. Later during the study we found out that the hMSCs were of male origin. As male cells express not only UTX but also UTY, which is located on the Y chromosome and which is known to have many corresponding properties, it would be more rational to elucidate the effect of UTX knockdown in female cells or to do a simultaneous knockdown of UTX an UTY in male cells (Walport, et al., 2014).

These results, altogether, suggested that H3K27me3 demethylation has a fatal role in fate decisions and more importantly might act as a switch by directing MSC differentiation towards adipocyte lineage at the expense of osteoblastogenesis. However, this needs further careful investigation. In vivo studies with conditional knockout of JMJD3 and/or UTX-UTY in MSCs could in fact further enlighten the function of histone H3K27 demethylation in lineage commitment of these cells.

Notably, our findings contradicted the two studies published by Ye et al. (Ye, et al., 2012) and Hemming et al. (Hemming, et al., 2014) where the authors demonstrated the osteoblast promoting function of JMJD3. Ye et al demonstrated that upon BMP 4 and 7 induced differentiation of hMSCs, demethylases JMJD2 (KDM4B), targeting H3K9me3/H3K36me3 and JMJD3 (KDM6B) were highly expressed during osteogenic differentiation. They attributed the osteogenic function of these demethylases due to direct demethylation of H3K27me3 and H3K9me3 from the promoter of early osteoblast marker genes DLX (including DLX2, DLX3, DLX5 and DLX6) and HOX6-1, HOXA10, HOXB2 and HOXC10. Moreover, Hemming et al, revealed direct targeting of RUNX2 promoter by UTX which also displayed osteoblast inducing role during the differentiation of MSCs.

The differences in the observations of these two studies with ours could be partly explained by the different origin of MSCs and variation of time span for differentiation. Namely, Ye et al. performed the experiments on primary human and mouse bone marrow MSCs whereas Hemming et al. used mortal bone marrow derived MSCs which might lose their stem cell and phenotypic properties after a number of cell divisions. Moreover, we only used shorter time points for differentiation studies to assess the earlier effects of JMJD3 in differentiation regulation whereas the differentiation time periods of Ye et al. were set to 3 weeks and 4 weeks for Hemming et al. Furthermore, they restricted their studies to few specific genes, whereas we performed transcriptome wide analysis of gene expression regulation by JMJD3.

Importantly, further investigation in the interaction of the two counterparts EZH2, responsible for methylation of H3K27me3 and the demethylases JMJD3/UTX needs to be done to understand regulation mechanisms completely. Recent work investigated the role of EZH2 in adipogenesis in mice (Wang, et al., 2010). I could be shown that due to direct repression of several Wnt genes, which are known to play a critical role in tissue homeostasis and developmental processes (Logan & Nusse, 2004), adipogenesis was increased. Regarding osteogenesis Dudakovic et al. demonstrated that histone methyltransferase EZH2 is

downregulated while differentiation of adipocyte derived MSC's into osteoblasts. Inhibiton of this enzyme led to a decrease of osteogenic differentiation and to a suppression of adipocyte differentiation (Dudakovic, et al., 2015).

In our study JMJD3 knockdown in general resulted in the downregulation of genes involved cell proliferation, DNA replication and cell division upon JMJD3 knockdown also pointed to its neoplastic properties. In fact studies from different groups have shown that dysregulation of JMJD3 and UTX are linked to oncogenesis in different tissues which makes them to an interesting target in cancer therapy (Willams, et al., 2014; Morozov, et al., 2017; Ntziachristos, et al., 2014).

Furthermore our transcriptome wide studies revealed that beneath upregulation of cell death, signaling transduction of p53 was increased in adipocytes upon JMDJ3 depletion. P53 which is also named the "guardian of the genome" is a tumor suppressor and plays not only a role in cancer development but also in many other cellular processes and in differentiation (Lane, 1992). It is presumed that p53 has an inhibitory effect on white adipocyte and on osteoblast differentiation (Molchadsky, et al., 2008). Furthermore it was found that it has regulatory effect on brown adipocyte differentiation and has a protective role against diet-induced obesity (Molchadsky, et al., 2013). According to our findings, JMJD3 could play a role in suppression of p53 signaling and therefore take part in regulation of MSC differentiation and metabolism processes.

In conclusion, we found that the H3K27me3 demethylases JMJD3 and UTX play important roles in MSC differentiation. The current study progresses our understanding of epigenetic regulation of cell fate choice in MSCs. The identification of the role of JMJD3 leading to increased osteoblastogenesis when depleted, was unexpected. A possible explanation could be that there might be a regulator of differential progresses above that level which gains relevance due to inhibition/knockdown of these demethylases. For a better understanding of these processes, investigation of upstream regulators and side-effects of JMDJ3/UTX regulation needs to be done.

Nevertheless these findings could become critical for the development of novel therapeutic strategies in tissue development and in the treatment of osteopathologies like osteoporosis. Inhibitors such as GSKJ-4, which we used in our studies can become important tools in the field of epigenetic therapies, a field that will presumably develop rapidly in medicine, especially in hematology and oncology. Nevertheless, more investigation about epigenetic and genetic changes in vivo need to be done before therapies become safe and practicable enough to establish them in widespread fields in medicine.

Summary

Epigenetic regulation plays a central role in controlling cell phenotype of stem cells. In this work we could show the importance of H3K27me3 demethylases JMJD3 and UTX in cell fate choice of human mesenchymal stem cells.

In particular we were able to demonstrate that due to active demethylation of H3K27 via the known histone demethylases JMJD3 and UTX MSC differentiation is altered in different manner. Whereas depletion of JMJD3 promoted cell differentiation into osteoblasts, UTX showed opposite effects. Promotion of osteoblast differentiation upon JMJD3 knockdown could be visualize with Alkaline phosphatase staining and validated by gene expression studies.

In adipogenesis gene expression of adipocyte specific genes was predominantly decreased upon JMJD3 and UTX knockdown. In contrast in Oil Red O staining we could observe clearly an increase of lipid droplet formation in UTX depleted samples.

By the use of a specific small-molecule inhibitor of H3K27me3 demethylases JMJD3 and UTX, named GSK-J4 we could show again a promoting effect on osteoblast differentiation at mRNA level.

In transcriptome wide gene analysis we could embed our previous findings in an overall picture of the role of JMJD3 in differentiation of MSCs. In Gene Ontology pathway analysis JMJD3 depletion led to upregulation of genes related to tissue development and cell locomotion confirming the important role in growth, regeneration and renewal. Furthermore ossification and lipid metabolism related genes were upregulated upon JMJD3 depletion in osteoblasts as well. Genes related to cell division, nuclear division and cell cycle were downregulated upon JMJD3 knockdown in all three conditions.

Our results progresses our understanding of epigenetic regulation of MSC differentiation and shows up new aspects. In particular it was unexpected that H3K27me3 demethylases JMJD3 and UTX did not suppress MSC differentiation when depleted, especially in osteoblasts. This indicates that there could be a regulator of differential progresses above that level which gains relevance due to inhibition/knockdown of these demethylases. More investigation in these progresses needs to be done to understand the role of JMJD3 and UTX completely.

Zusammenfassung

Epigenetische Regulationsmechanismen spielen eine zentrale Rolle in der Kontrolle des Phänotyps mesenchymaler Stammzellen. In dieser Arbeit konnten wir den Einfluss von JMJD3 und UTX, zweier H3K27me3 Demethylasen auf die Differenzierung humaner mesenchymaler Stammzellen in Adipozyten und Osteoblasten demonstrieren.

Es gelang uns darzustellen, dass die Differenzierung der MSCs durch JMJD3 und UTX in unterschiedlicher Weise beeinflusst wird. Durch Färbungen der Alkalischen Phosphatase und Geneexpressionsanalysen mittels Real-Time PCR zeigte sich, dass der Knockdown von JMJD3 zu einer gesteigerten Differenzierung von Osteoblasten führt. Beim Knockdown von UTX sahen wir gegenteiligen Effekt.

Durch den Einsatz von GSK-J4, einen für JMJD3 und UTX spezifischen Inhibitor, konnten wir wiederholt eine Zunahme der Osteoblasten-spezifischen Genexpression demonstrieren.

Die Analyse Adipocyten-spezifischer Gene zeigte eine Abnahme der Expression durch das Ausschalten von JMJD3 und UTX durch entsprechende siRNA. Demgegenüber beobachteten wir in der ‚Oil Red O' Färbung eine klare Zunahme der gefärbten Lipid Tröpfchen durch den Knockdown von UTX.

Mittels Transkriptom-Analyse konnten wir ein Gesamtbild des Einflusses von JMJD3 auf MSCs und deren Differenzierung generieren. Mit Hilfe der ‚Gene Ontology pathway' Analyse zeigten wir, dass der Knockdown von JMJD3 unter anderem zu einer Hochregulierung von Genen führt welche eine wichtige Rolle in der Entwicklung von Geweben und Zellbewegung tragen. Darüber hinaus war die Expression relevanter Gene für Ossifikation und den Fettstoffwechsel in zu Osteoblasten differenzierten MSCs gesteigert. Gene welche in Beziehung zur Zell- und Zellkernteilung, sowie zum Zellzyklus stehen waren in allen drei Konditionen (undifferenziert, Adipozyten, Osteoblasten) runter reguliert.

Diese Arbeit zeigt neue Aspekte epigenetischer Regulationsmechanismen mesenchymaler Stammzellen auf. Insbesondere die H3K27me3 Demethylase JMJD3 zeigt unerwarteter Weise einen divergenten Einfluss auf die Differenzierung von Osteoblasten und Adipozyten welcher so nicht vorbeschrieben war. Ob weitere ‚Upstream' Regulatoren die Ausdifferenzierung von MSCs begünstigen beziehungsweise hemmen oder ob durch die Inhibition/den Knockdown von JMJD3 ein Ungleichgewicht zu Gunsten von anderen Demethylasen/Methyltransferasen oder Transkriptionsfaktoren besteht, muss in weiteren Experimenten untersucht werden um ein vollständiges Verständnis der Abläufe zu erlangen.

References

Agger, K. et al., 2007. *UTX and JMJD3 are histone H3K27 demethylases involved in HOX gene regulation and development.* s.l.:Nature 449: 731-4.

Alberts, B. et al., 2002. *Molecular Biology of the Cell. 4th edition..* s.l.:Garland Science.

Anders, S., Pyl, P. & Huber, W., 2015. *HTSeq--a Python framework to work with high-throughput sequencing data..* s.l.:Bioinformatics 31(2), 166-169.

Babraham Bioinformatics, [Stand 04.02.2019, 14:35]. *FastQC A Quality Control tool for High Throughput Sequence Data,* [Online im internet]: URL: http://www.bioinformatics.babraham.ac.uk/projects/fastqc.

Barski, A. et al., 2007. *High-Resolution Profiling of Histone Methylations in the Human Genome.* s.l.:Cell Volume 129, Issue 4, pp. 823-837.

Bartholomew, A., Sturgeon, C. & Siatskas, M., 2002. *Mesenchymal stem cells suppress lymphocyte proliferation in vitro and prolong skin graft survival in vivo..* s.l.:Experimental Hematology, Vol. 30, No. 1, pp. 42–48.

Beckermann, B. et al., 2008. *VEGF expression by mesenchymal stem cells contributes to angiogenesis in pancreatic carcinoma.* s.l.:Br. J. Cancer, 99, pp. 622–631.

Bedi, U. et al., 2014. *SUPT6H controls estrogen receptor activity and cellular differentiation by multiple epigenomic mechanisms..* s.l.:Oncogene 34, 465-473.

Bennett, C. et al., 2002. *Regulation of Wnt signaling during adipogenesis.* s.l.:J. Biol Chem 277: 30998-31004.

Bernstein, B. et al., 2006. *A bivalent chromatin structure marks key developmental genes in embryonic stem cells.* s.l.:Cell 125: 315–326.

Blankenberg, D. et al., 2010. *Manipulation of FASTQ data with Galaxy..* s.l.:Bioinformatics; 26(14) pp. 1783-5.

Blankenberg, D. et al., 2010. *Galaxy: a web-based genome analysis tool for experimentalists..* s.l.:Current Protocols in Molecular Biology ; Chapter 19, Unit 19.10.1-21.

Boucher, J., Tseng, Y. & Kahn, C., 2010. *Insulin and Insulin-like Growth Factor-1 Receptors Act as Ligand-specific Amplitude Modulators of a Common Pathway Regulating Gene Transcripion.* 285(22): 17235-17245 ed. s.l.:J Biol Chem.

Boyer, L. et al., 2006. *Polycomb complexes repress developmental regulators in murine embryonic stem cells..* s.l.:Nature 441(7091), pp. 349-353.

Burgold, T. et al., 2008. *The histone H3 lysine 27-specific demethylase Jmjd3 is required for neural commitment..* s.l.:PLoS One 3(8): e3034.

Cao, R. et al., 2002. *Role of hisoe H3 lysine 27 methylation in Polycomb-group silencing.* s.l.:Science 298: 1039-1043.

Caplan, A., 1991. *Mesenchymal stem cells.* s.l.:J. Orthop. Res. 9, 641–650 .

Chang, C. et al., 2011. *EZH2 Promotes Expansion of Breast Tumor Initiating Cells through Activation of RAF1-β-Catenin Signaling.* s.l.:Cancer Cell, Volume 19, Issue 1, p86-100.

Cheng, G., Deng, C. & Li, Y., 2012. *TGF-beta and BMP signaling in osteoblast differentiation and bone formation..* s.l.:International Journal of Biological Science; 8: 272–288..

Chen, S. et al., 2012. *The histone H3 Lys 27 demethylase JMJD3 regulates gene expression by impacting transcriptional elongation.* s.l.:Genes & Dev. 26: 1364-1375.

Corcione, A. et al., 2006. *Human mesenchymal stem cells modulate B-cell functions..* s.l.:Blood: 107 (1) pp. 367-372.

De Santa, F. et al., 2007. *The histone H3 lysine-27 demethylase Jmjd3 links inflammation to inhibition of polycomb-mediated gene silencing.* s.l.:Cell 130(6): 1083-1094.

Dominici, M. et al., 2006. *Minimal criteria for defining multipotent mesenchymal stromal cells. The International Society for Cellular Therapy position statement.* s.l.:Cytotherapy Vol. 8, No. 4, 315-317.

Dubuc, A. et al., 2013. *Aberrant patterns of H3K4 and H3K27 histone lysine methylation occurs across subgroups in medulloblastoma.* s.l.:Acta Neuropathol 125: 373-384.

Ducy, P. et al., 1997. *Osf2/Cbfa1: a transcriptional activator of osteoblast differentiation..* s.l.:Cell 89(5), pp. 747-754.

Dudakovic, A. et al., 2015. *Epigenetic Control of Skeletal Development by the Histone Methyltransferase Ezh2.* 290;46;27604-27617 ed. s.l.:J. Biol. Chem..

Estarás , C. et al., 2013. *RNA polymerase II progression through H3K27me3-enriched gene bodies requires JMJD3 histone demethylase.* s.l.:Mol. Biol. Cell 24: 351-360.

Ferrari, K. J. et al., 2014. *Polycomb-Dependent H3K27me1 and H3K27me2 Regulate Active Transcription and Enhancer Fidelity.* s.l.:Molecular Cell Volume 53, Issuer 1, pp. 49-62.

Friedenstein, A. J. P.-S. & Petrakova, K., 1966. *Osteogenesis in transplants of bone marrow cells..* s.l.:The Journal of Embryological Experimental Morphology, 16; pp. 381–390.

Giardine, B. et al., 2005. *Galaxy: A platform for interactive large-scale genome analysis..* s.l.:Genome Research 15; pp. 1451-1455 .

Goecks, J., Nekrutenko, A. & Taylor, J., 2010. *Galaxy: a comprehensive approach for supporting accessible, reproducible, and transparent computational research in the life sciences..* s.l.:Genome Biology; 11(8): R86.

Gomes, N. et al., 2006. *Gene-specific requirement for P-TEFb activity and RNA polymerase II phosphorylation within p53 transcriptional program..* s.l.:Genes Dev. 20, 601-612.

Gonzalez, M. E. et al., 2009. *Downregulation of EZH2 decreases growth of estrogen receptor-negative invasive breast carcinoma and requires BRCA1.* s.l.:Oncogene 28, pp. 843-853.

Greenfield, A. et al., 1998. *The UTX gene escapes X inactivation in mice and humans.* s.l.:Hum Mol genet. 7:737-742.

Gregoire, F., Smas, C. & Sul HS, 1998. *Understanding adipocyte differentiation.* s.l.:Physiol Rev. 78(3): 783-809.

Gui, Y. et al., 2011. *Frequent mutations of chromatin remodeling genes in transitional cell carcinoma of the bladder..* s.l.:Nature Genetics 43: 875–878.

Hadji , P. et al., 2013. *The epidemiology of osteoporosis--Bone Evaluation Study (BEST): an analysis of routine health insurance data.* s.l.:Deutsches Ärtzeblatt 110(4): 52-57.

Haiyan, H. et al., 2009. *BMP signaling pathway is required for commitment of C3H10T1/2 pluripotent stem cells to the adipocyte lineage.* 106: 12670-12675 ed. s.l.:Natl Acad Sci USA.

Hemming, S. et al., 2014. *EZH2 and KDM6A act as an epigenetic switch to regulate mesenchymal stem cell lineage specification..* s.l.:Stem Cells. 10.1002/stem.1573..

Horton, J. et al., 2010. *Enzymatic and structural insights for substrate specificity of a family of jumonji histone lysine demethylases.* s.l.:Nat Struct Mol Biol 17: 38–43.

Huszar , J. M. & Payne, C. J., 2014. *MIR146A inhibits JMJD3 expression and osteogenic differentiation in human mesenchymal stem cells..* s.l.:FEBS letters 588(9):1850-6.

Jenuwein, T. & Allis, C., 2001. *Translating the histone code..* s.l.:Science; 293(5532): 1074-80..

Johnsen, S., 2012. *CDK9 and H2B Monoubiquitination: A Well-Choreographed Dance..* s.l.:PLoS Genet.; 8(8):e1002860.

Jung, Y. et al., 2013. *Recruitment of mesenchymal stem cells into prostate tumours promotes metastasis.* s.l.:Nat. Commun., 4, p. 1795.

Karnoub, A. et al., 2007. *Mesenchymal stem cells within tumour stroma promote breast cancer metastasis.* s.l.:Nature, 449 (2007), pp. 557–563.

Karpiuk, O. et al., 2012. *The histone H2B monoubiquitination regulatory pathway is required for differentiation of multipotent stem cells..* s.l.:Mol. Cell. 46(5): 705-13.

Kassis, I. et al., 2006. *Isolation of mesenchymal stem cells from G-CSF-mobilized human peripheral blood using fibrin microbeads..* s.l.:Bone Marrow Transplant 37: 967-976.

Kim, D. et al., 2013. *TopHat2: accurate alignment of transcriptomes in the presence of insertions, deletions and gene fusions..* s.l.:Genome Biology 14:R36.

Kim, W. et al., 2010. *Hedgehog signaling and osteogenic differentiation in multipotent bone marrow stromal cells are inhibited by oxidative stress..* s.l.:Journal of Cellular Biochemistry; 111: 1199–1209..

Kleer, C. G. et al., 2003. *EZH2 is a marker of aggressive breast cancer and promotes neoplastic transformation of breast epithelial cells.* s.l.:Proceedings of the National Academy of Science of the USA 100, pp. 11606–11611.

Komori, T., 2005. *Regulation of Skeletal Development by the Runx Family..* s.l.:Journal of Cellular Biochemistry 95:445–453.

Komori, T., 2010. *Regulation of osteoblast differentiation by Runx2..* s.l.:Advances in Experimental Medicine and Biology; 658: 43–49..

Kornberg, R., 1974. *Chromatin Structure: A Repeating Unit of Histones and DNA..* s.l.:Science 184, pp. 868-871.

Kouzarides, T., 2007. *Chromatin modifications and their function. Cell 128, 693-705..* s.l.:Cell 128, pp. 693-705.

Kruidenier, L. et al., 2012. *A selective jumonji H3K27 demethylase inhibitor modulates the proinflammatory macrophage response..* s.l.:Nature 488, 404–408..

Kuzmichev, A. et al., 2002. *Histone methyltransferase activity associated with a human multiprotein complex containing the Enhancer of Zeste protein.* s.l.:Genes Dev. 16: 2893-2905.

Lane, D., 1992. *p53, guardian of the genome.* s.l.:Nature; 358, p.15-16.

Lan, F. et al., 2007. *A histone H3 lysine 27 demethylase regulates animal posterior development..* s.l.:Nature. Oct 11;449(7163):689-94..

Lan, F. et al., 2007. *A histone H3 lysine 27 demethylase regulates animal posterior development..* s.l.:Nature 449: 689-694.

Le Blanc, K., Rasmusson, I., Sundberg, B. & et al., 2004. *Treatment of severe acute graft-versus-host disease with third party haploidentical mesenchymal stem cells..* s.l.:Lancet, Vol. 363, No. 9419, pp. 1439–1441.

Lee, M. et al., 2007. *Demethylation of H3K27 Regulates Polycomb Recruitment and H2A Ubiquitination.* s.l.:Science 318: 447-450.

Lee, S., Lee, J. & Lee, S., 2012. *UTX, a histone H3-lysine 27 demethylase, acts as a critical switch to activate the cardiac developmental program..* s.l.:Developmental Cell 22(1), pp. 25-37.

Lewis, B. P., Burge, C. B. & Bartel, D. P., 2005. *Conserved seed pairing, often flanked by adenosines, indicates that thousands of human genes are microRNA targets..* s.l.:Cell 120(1):15-20.

Lin, G. & Hankenson, K., 2011. *Integration of BMP, Wnt, and notch signaling pathways in osteoblast differentiation..* s.l.:Journal of Cellular Biochemistry; 112: 3491–3501..

Logan, C. & Nusse, R., 2004. *The Wnt signaling pathway in development and disease..* 20:781-810 ed. s.l.:Annuv Rev Cell Dev Biol.

Love, M., Huber, W. & Anders, S., 2014. *Moderated estimation of fold change and dispersion for RNA-seq data with DESeq2..* s.l.:Genome Biology 11, R14.

Mello, M., 1983. *Cytochemical properties of euchromatin and heterochromatin..* s.l.:The Histochemical Journal Vol. 15, No. 8, pp. 739-751.

Messer, H., Jacobs, D., Dhummakupt, A. & Bloom DC, 2015. *Inhibition of H3K27me3-specific histone demethylases JMJD3 and UTX blocks reactivation of herpes simplex virus 1 in trigeminal ganglion neurons..* s.l.:Journal of Virology, 89(6): 3417-20.

Mikkelsen, T. et al., 2007. *Genome-wide maps of chromatin state in pluripotent and lineage-committed cells..* s.l.:Nature; 448(7153):553-60..

Miyake , N. et al., 2013. *MLL2 and KDM6A mutations in patients with Kabuki Syndrome.* s.l.:Am J Med Genet Part A 61A: 2234–2243.

Molchadsky, A. et al., 2013. *p53 is required for brown adipogenic differentiation and has a protective role against diet-induced obesity.* s.l.:Cell Death and Differentiation, 20(5) p.774-783.

Molchadsky, A. et al., 2008. *p53 Plays a Role in Mesenchymal Differentiation Programs, in a Cell Fate Dependent Manner.* s.l.:PLoS ONE, 3(11): e3707.

Morozov, V. M., Li, Y., Clowers, M. M. & Ishov, A. M., 2017. Inhibitor of H3K27 demethylase JMJD3/UTX GSKJ-4 is a potential therapeutic option for castration resistant prostate cancer.. *Oncotarget*, Issue 8 (37): 62131-62142.

Muller, J. et al., 2002. *Histone methyltransferase activity of Drosophila Polycomb group repressor complex.* s.l.:Cell 111: 197-208.

Nakashima , K. et al., 2002. *The Novel Zinc Finger-Containing Transcription Factor Osterix Is Required for Osteoblast Differentiation and Bone Formation..* s.l.:Cell; 108: 17–29..

Nicola, M., Carlo-Stella, C. & Magni, M., 2002. *Human bone marrow stromal cells suppress T-lymphocyte proliferation induced by cellular or nonspecific mitogenic stimuli..* s.l.:Blood, Vol.99, No. 10 pp. 3838-3843.

Noer, A., Lindeman, L. & Collas, P., 2009. *Histone H3 modifications associated with differentiation and long-term culture of mesenchymal adipose stem cells.* s.l.:Stem Cells Dev. 18, 725–736..

Ntziachristos, P. et al., 2014. Contrasting roles oh histone 3 lysine demethylases in acute lymphoblastic leukaemia.. *Nature*, Issue 514(7523):513-7.

Pan, G. et al., 2007. *Whole-genome analysis of histone H3 lysine 4 and lysine 27 methylation in human embryonic stem cells..* s.l.:Cell Stem Cell 1: 299–312.

Picard Tools, [Stand 04.02.2019, 17:40]. *http://broadinstitute.github.io/picard/,* s.l.: [Online im Internet].

Pino, A., Rosen, C. & Rodríguez, J., 2012. *In osteoporosis, differentiation of mesenchymal stem cells (MSCs) improves bone marrow adipogenesis..* s.l.:Biological Research 45(3), pp. 279-287.

Pittenger, M., 1999. *Multilineage potential of adult human mesenchymal stem cells.* s.l.:Science. 284:143–147.

Pollina, E. & Brunet, A., 2011. *Epigenetic regulation of aging stem cells..* s.l.:Oncogene; 30, 3105–3126..

Roh, T., Cuddapah, S., Cui, K. & Zhao, K., 2006. *The genomic landscape of histone modifications in human T cells..* s.l.:Proceedings of the National Academy of Science of the United States of America.

Rosen, E. et al., 1999. *PPAR gamma is required for the differentiation of adipose tissue in vivo and in vitro..* s.l.:Molecular Cell; 4(4):611-7..

Sato, M. et al., 1998. *Transcriptional regulation of osteopontin gene in vivo by PEBP2alphaA/CBFA1 and ETS1 in the skeletal tissues..* s.l.:Oncogene 17(12):1517-25..

Saurin, A. et al., 2001. *A Drosophila Polycomb group complex includes Zeste and dTAFII proteins.* s.l.:Nature 412: 655-660.

Schuettengruber , B. et al., 2007. *Genome regulation by polycomb and trithorax proteins.* s.l.:Cell 128:735-45.

Schuettengruber, B., Martinez, A., Iovino, N. & Cavalli , G., 2011. *Trithorax group proteins: switching genes on and keeping them active.* s.l.:Nat Rev Mol Cell Biol 12: 799-814.

Serakinci, N. et al., 2011. *Mesenchymal stem cells as therapeutic delivery vehicles targeting tumor stroma.* s.l.:Cancer Biother Radiopharm, 26 (6) , pp. 767-773.

Serakinci, N. et al., 2004. *Adult human mesenchymal stem cell as a target for neoplastic transformation..* s.l.:Oncogene 23: 5095–5098..

Shao, Z. et al., 1999. *Stabilization of chromatin structure by PRC1, a Polycomb-complex.* s.l.:Cell 98: 37-46.

Shinagawa, K. et al., 2010. *Mesenchymal stem cells enhance growth and metastasis of colon cancer.* s.l.:Int. J. Cancer, 127 (2010), pp. 2323–2333.

Shpargel, K., Sengoku, T., Yokoyama, S. & Magnuson, T., 2012. *UTX and UTY Demonstrate Histone Demethylase-Independent Function in Mouse Embryonic Development.* s.l.:PLoS Genetics 8(9):e1002964.

Shumaker, D. et al., 2006. *Mutant nuclear lamin A leads to progressive alterations of epigenetic control in premature aging..* s.l.:Proceedings of the National Academy of Science; 103, 8703–8708..

Simon, J. & Kingston RE, 2009. *Mechanisms of polycomb gene silencing: knowns and unknowns.* s.l.:Nat Rev Mol Cell Biol. 10: 697-708.

Simonsen, J. et al., 2002. *Telomerase expression extends the proliferative life-span and maintains the osteogenic potential of human bone marrow stromal cells..* 20(6):592-6 ed. s.l.:Nat Biotechnol..

Strahl, B. & Allis, C., 2000. *The language of covalent histone modifications..* s.l.:Nature 403, pp. 41-45.

Suspek, F., Bošnjak, M., Škunca, N. & Šmuc, T., 2011. *REVIGO Summarizes and Visualizes Long Lists of Gene Ontology Terms..* s.l.:PLoS ONE 6, e21800.

Tang, Q. & Lane, M., 2012. *Adipogenesis: from stem cell to adipocyte..* s.l.:Annual Review of Biochemestry; 81: 715–736..

van Haaften, G. et al., 2009. *Somatic mutations of the histone H3K27 demethylase gene UTX in human cancer.* s.l.:Nat Genet 41: 521-523.

Varambally, S. et al., 2002. *The polycomb group protein EZH2 is involved in progression of prostate cancer.* s.l.:Nature 419, pp. 624-629.

Veryasov, V. et al., 2014. *Isolation of mesenchymal stromal cells from extraembryonic tissues and their characteristics..* s.l.:Bulletin of experimental biology and medicine 157(1): 119-124.

Visser, H. et al., 2001. *The Polycomb group protein EZH2 is upregulated in proliferating, cultured human mantle cell lymphoma..* s.l.:British Journal of Haematology; 112(4):950-8..

Voigt, P., Wee-Wei, T. & Reinberg, D., 2013. *A double take on bivalent promoters.* s.l.:Genes & Dev. 27: 1318-1338.

Wagner, W. et al., 2005. *Comparative characteristics of mesenchymal stem cells from human bone marrow, adipose tissue, and umbilical cord blood..* s.l.:Exp. Hematology 33: 1402-1416.

Walport, L. et al., 2014. *Human UTY (KDM6C) is a male-specific Ne-methyl lysyl demethylase..* 289(26): 18302-18313 ed. s.l.:J Biol Chem..

Wang, L. et al., 2010. *Histone H3K27 methyltransferase Ezh2 represses Wnt genes to facilitate adipogenesis.* 107;No.16; 7317-7322 ed. s.l.:PNAS.

Warnes, G. et al., [Stand: 04.02.2019, 15:33]. *Various R Programming Tools for Plotting Data.* [Online] Available at: https://cran.r-project.org/web/packages/gplots/gplots.pdf

Wei, Y. et al., 2011. *CDK1-dependent phosphorylation of EZH2 suppresses methylation of H3K27 and promotes osteogenic differentiation of human mesenchymal stem cells..* s.l.:Nature Cell Biology 13, pp. 87-94.

Wei, Y. et al., 2008. *Loss of Trimethylation at Lysine 27 of Histone H3 Is a Predictor of Poor Outcome in Breast, Ovarian, and Pancreatic Cancers.* s.l.:Molecular Carcinogenesis 47(9), pp. 701-706.

Widom, J., 1998. *Structure, dynamics, and function of chromatin in vitro..* s.l.:Annual review of biophysics and biomolecular structure Vol. 27, pp. 285-327.

Willams, K. et al., 2014. The histone lysine demethylase JMJD3/KDM6B is recruited to p53 bound promoters and enhancer elements in a p53 dependent manner.. *PLoS One*, Issue 9:e96545.

Wu, Z. et al., 2011. *Polycomb protein EZH2 regulates cancer cell fate decision in response to DNA damage..* s.l.:Cell Death Differentiation, 18, p1771-1779.

Xiao-Xia, J. et al., 2005. *Human mesenchymal stem cells inhibit differentiation and function of monocyte-derived dendritic cells..* s.l.:Blood: 105 (10), pp. 4120- 4126 .

Ye, L. et al., 2012. *Histone Demethylases KDM4B and KDM6B Promotes Osteogenic Differentiation of Human MSCs.* s.l.:Cell Stem Cell; 11 (1): 50-61.

Young, M., Wakefield, M., Smyth, G. & Oshlack, A., 2010. *Gene ontology analysis for RNA-seq: accounting for selection bias..* s.l.:Genome Biology 11., R14.

Zheng, H. et al., 2004. *Cbfa1/osf2 transduced bone marrow stromal cells facilitate bone formation in vitro and in vivo..* s.l.:Calcif Tissue Int.; 74(2):194-203..

Abbreviations

ALPL – Alkaline phosphatase gene

BGLAP – Bone gamma-carboxyglutamic acid-containing protein

BMP – Bone morphogenetic proteins

CD – Cluster of differentiation

DEPC – Diethylpyrocarbonate

DNA – Deoxyribonucleic acid

dNTP – Deoxynucleotide

DMEM – Dulbecco's Modified Eagle's Medium

EDTA – Ethylenediaminetetraacetic acid

EED – Embryonic ectoderm development

ESC – Embryonic stem cell

EtOH – Ethanol

EZH2 – Enhancer of Zeste 2

FBS – Fetal bovine serum

G6PD – Glucose-6-phosphate dehydrogenase

GAPDH – Glyceraldehyde 3-phosphate dehydrogenase

H3K4 (me3) – Histone H3 Lysine 4 (trimethylation)

H3K9 – Histone H3 Lysine 9

H3K27 (me3) – Histone H3 Lysine 27 (trimethylation)

H3K36 – Histone H3 Lysine 36

H3K79 – Histone H3 Lysine 79

H4K20 – Histone H4 Lysine 20

HGPS – Hutchinson-Gilford progeria syndrome

HLA-DR – Human leukocyte antigen-D-related

hMSCs – Human mesenchymal stem cells

HNRNPK – Heterogeneous nuclear ribonucleoprotein K

HRP – Horseradish peroxidase

IBMX – 3-isobutyl-1-methylxanthine

IL – Interleukin

i.e. – id est

JMJD3 – Jumonji domain containing 3

KDM6A/B – Lysine (K)-Specific Demethylase 6A/B

LPL – Lipoproteinlipase

MEM – Minimum Essential Medium Eagle

MLL - Mixed-lineage leukemia protein 2

mRNA – Messenger RNA

MSC – Mesenchymal stem cell

PcG – Polycomb-group proteins

PDK4 – Pyruvate dehydrogenase lipoamide kinase isozyme 4

PHD – Plant homeodomain

PPARG – Peroxisome proliferator-activated receptor gamma

PRC1/2 – Polycomb repressive complex 1/2

RASD1 – Dexamethasone-induced Ras-related Protein 1

RbAp48 – Retinoblastoma binding protein 4

RIPA – Radioimmunoprecipitation assay buffer

RNA – Ribonucleic acid

RUNX2 – Runt-related transcription factor 2

SDS – Sodium dodecyl sulfate

siRNA – Small interfering RNA

SUZ12 – Suppressor of zeste 12

TBST - Tris-Buffered Saline and Tween 20

TERT – Telomerase reverse transcriptase

Tris – Tris(hydroxymethyl)aminomethane

TrxG - Trithorax Group

UTX – Ubiquitously transcribed tetratricopeptide repeat, X chromosome

Acknowledgement

Ich möchte mich zuerst und vor allem bei meinem Betreuer Prof. Dr. S. A. Johnsen bedanken für die Chance meine Dissertation in seiner Laborgruppe durchzuführen, sowie für die wissenschaftliche und menschliche Unterstützung während der gesamten Zeit des Projektes.
Ich bin dankbar für Herausforderungen vor die ich gestellt wurde und die Erfahrungen die ich sammeln konnte, für inspirierende Diskussionen und eine gute Stimmung im gesamten Arbeitsumfeld.

Insbesondere möchte ich Dr. Z. Najafova für ihre Hilfe, ihre Ratschläge und Geduld während des gesamten Projektes danken. Durch ihre zielstrebige, exakte und außerordentlich umsichtige Art und Arbeitsweise ist sie eine große Inspiration für mich gewesen.

Weiterhin danke ich Prof. Dr. K. Pantel für die Möglichkeit, dass ich meine Arbeit im Institut für Tumorbiologie durchführen konnte und für die Bereitwilligkeit meine Dissertation zu begutachten.

Zu guter Letzt danke ich meiner Familie und meinen Freunden, sowie meinen Kollegen die mich fortwährend ermutigt und unterstützt haben und bei denen ich jederzeit Rückhalt und Verständnis erfahren habe.

Hinweis: Der Lebenslauf wurde aus datenschutzrechtlichen Gründen entfernt

Statutory declaration

Ich versichere ausdrücklich, dass ich die Arbeit selbständig und ohne fremde Hilfe verfasst, andere als die von mir angegebenen Quellen und Hilfsmittel nicht benutzt und die aus den benutzten Werken wörtlich oder inhaltlich entnommenen Stellen einzeln nach Ausgabe (Auflage und Jahr des Erscheinens), Band und Seite des benutzten Werkes kenntlich gemacht habe.
Ferner versichere ich, dass ich die Dissertation bisher nicht einem Fachvertreter an einer anderen Hochschule zur Überprüfung vorgelegt oder mich anderweitig um Zulassung zur Promotion beworben habe.

Ich erkläre mich einverstanden, dass meine Dissertation vom Dekanat der Medizinischen Fakultät mit einer gängigen Software zur Erkennung von Plagiaten überprüft werden kann.

Unterschrift: .....